International Journal of Robotics and Automation (IJRA)
Vol. 3, No. 1, March 2014, pp. 13 – 29
ISSN: 2089-4856

Global Tracking Control of Quadrotor VTOL Aircraft in Three-Dimensional Space

K. D. Do
Department of Mechanical Engineering, Curtin University, Perth, WA 6845, Australia

Article Info

Article history:
Received Jul 3, 2013
Revised Dec 15, 2013
Accepted Jan 10, 2014

Keyword:
Global tracking
quadrotor aircraft
one-step ahead backstepping
Lyapunov's direct method
exponential observers

ABSTRACT

This paper presents a method to design controllers that force a quadrotor vertical take-off and landing (VTOL) aircraft to globally asymptotically track a reference trajectory in three-dimensional space. Motivated by the vehicle's steering practice, the roll and pitch angles are considered as immediate controls plus the total thrust force provided by the aircraft's four rotors to control the position and yaw angle of the aircraft. The control design is based on the newly introduced one-step ahead backstepping, the standard backstepping and Lyapunov's direct methods. A combination of Euler angles and unit-quaternion for the attitude representation of the aircraft is used to obtain global tracking control results. The paper also includes a design of observers that exponentially estimate the aircraft's linear velocity vector and disturbances. Simulations illustrate the results.

Corresponding Author:
K.D. Do
Department of Mechanical Engineering, Curtin University
Kent Street, Perth, WA 6845, Australia
Phone: +61 892667577
Email: duc@curtin.edu.au

1. INTRODUCTION

Quadrotor aircraft are attractive VTOL aerial vehicles for various military and civilian applications. A quadrotor aircraft usually has a rigid cross frame equipped with two pairs of rotors. These two pairs of rotors rotate in opposite direction in order to compensate the effect of the reactive torques. The flying mechanism of the aircraft is explained as follows. The vertical (heave) motion is resulted by collectively increasing and decreasing the speed of all four rotors. The pitch and roll motions are achieved by changing the speed of the front-rear pair and the left-right pair of rotors, respectively. The yaw motion is realized by the different reactive torques between the two pairs of the rotors. Finally, the horizontal (surge and sway) motions are resulted from the coupling of the roll, pitch and vertical motions. There is no change in the direction of rotation of the rotors. The aforementioned flying mechanism implies that the motions of the quadrotor aircraft are nonlinearly coupled. Nonlinearities come from the fact that the equations describing the motions of the aircraft are nonlinear, see Subsection 2.1. for details. Moreover, the aircraft are underactuated since there are only four independent control inputs (four rotors) while there are six degrees of freedom (surge, sway, heave, roll, pitch, and yaw) to be controlled, see [?] for more details on controlling other underactuated mechanical systems. The underactuated and nonlinear coupling features of the quadrotor aircraft result in difficulties in controlling their motions.

Due to the aforementioned difficulties, controlling a VTOL aircraft was initially restricted in a vertical plane, i.e., the horizontal (surge and sway), pitch and yaw motions were ignored. An approximate input-output linearization approach was used in [?], [?], [?], [?], [?] to develop controllers for stabilization and output tracking/regulation of a VTOL aircraft. In [?], by noting that the output at a fixed point with respect to the aircraft body (Huygens center of oscillation) can be used, an interesting approach was introduced to design an output tracking controller. However, the proposed controller was not defined in the whole space. Simple approaches were developed in [?], [?] to provide global controllers for the stabilization and tracking control of a VTOL aircraft. A dynamic high-gain approach was used in [?] to design a controller to force the VTOL aircraft to globally practically track a reference trajectory.

Since the quadrotor aircraft usually operate in three-dimensional (3D) space, controlling all of their six degrees of freedom has recently attracted attention of researchers in the control and robotic communities. In comparison with the two-dimensional (2D) case mentioned above, controlling the aircraft in 3D space has two main additional challenges. The first one is that in the 2D case there are two independent control inputs while there are three outputs desirable to be controlled. The 3D case has four independent control inputs and six outputs desirable to be controlled. The second challenge is that there are singularities in the kinematic equations describing the motions of the aircraft if the Euler angles are used to represent the orientation (attitude) of the aircraft. A combination of feedback linearization [?], nested control design [?], and backstepping techniques [?] was proposed in [?], [?], [?] to design a stabilization and tracking controller for a quadrotor aircraft in 3D space. However, the result was local due to the use of Euler angles for representation of the quadrotor aircraft's attitude. To overcome the singularities due to the use of Euler angles for describing the aircraft's attitude, the unit-quaternion [?] was used. To relax the underactuated constraint of the quadrotor aircraft, several authors considered the attitude tracking problem and the position tracking one separately. In [?] and [?], the attitude control problem for the quadrotor aircraft was addressed. Control of the attitude is more straightforward than that of the position for the quadrotor aircraft because the dynamics of the attitude of the aircraft are fully actuated while the position dynamics are underactuated.

Motivated by the work in [?], the position tracking problem for the quadrotor aircraft was recently considered in [?] and [?]. In [?], the authors addressed the problem of position tracking for quadrotor aircraft without linear velocity measurement where the unmeasured linear velocity was handled by a dynamical approach in [?]. In [?], the position tracking problem for the aircraft subject to constant disturbances was solved. However, in both [?] and [?] the attitude was not controlled. This is because the authors of [?] and [?] treated an underactuated quadrotor as an over-actuated one in the position tracking problem to enable them to use an attitude extraction algorithm for extracting a desired part of the attitude. This means that in [?] and [?] four independent control inputs were used to control three outputs (position in 3D). Moreover, a serious problem without controlling the heading angle (a part of the attitude) is that the quadrotor can rotate around the vertical axis, i.e., the zero dynamics of the heading angle can be unstable. This problem was recognized in the field of controlling underactuated surface ships [?]. In contrast to the surface ships, the quadrotor aircraft are symmetric in the horizontal plane. Therefore, it is impossible to use the aft heavy property to prevent the quadrotor aircraft from rotating around the vertical axis with the position tracking control algorithms in [?] and [?]. The above findings motivate the contributions of this paper on proposing a new method to design a global tracking controller for the quadrotor aircraft. The paper's contributions include three folds.

1. A combination of the Euler angles and the unit-quaternion is used for representation of the quadrotor aircraft's attitude in the equations of motion of the aircraft. This combination allows us to design the tracking controller with a clear physical meaning, and to avoid singularities in the equations representing the aircraft's attitude. As such, the unit-quaternion is used for representation of the quadrotor aircraft's attitude to avoid singularities and the Euler angles are used to design the immediate controls that stabilize the position and yaw tracking errors. These immediate controls are then represented back by the unit-quaternion to avoid singularities. Therefore, the control design has a clear physical meaning and is straightforward to follow in the sense that the roll and pitch angles are used in combination with the heave velocity to control the un-actuated degrees of freedom (sway and surge). As such, the control algorithm in this paper controls both the position and the heading angle while ensures boundedness of the roll and pitch angles. Therefore, the problem of the quadrotor rotating around the vertical axis existing in [?] and [?] is avoided.

2. A new one-step ahead backstepping method is introduced. This method is used to design bounded immediate controls for the roll and pitch angles and heave velocity of the aircraft to control its horizontal motions. The one-step ahead backstepping method is applied to derive an explicit Lyapunov function, of which the derivative is negative definite, to design a global tracking control law. This results in a global asymptotic and local exponential stable closed loop system. Global asymptotic and local exponential stability of the closed loop is more desirable than only global asymptotic stability obtained in [?] and [?] (for only for position tracking) because local exponential stability results in certain robustness with respect to disturbances and fast convergence of the tracking errors to zero when these errors are sufficiently small. Since the one-step ahead backstepping technique is constructive and flexible, it is not restricted to an application in this paper but can be used for other control designs.

3. Observers are proposed to exponentially estimate the unmeasured linear velocity of the aircraft and disturbances, which can be time-varying. These observers can be then applied to the full-state feedback control design to result in controllers for tracking control of the aircraft without measurement of the linear velocity and with disturbances. In comparison with [?] and [?], since the observers exponentially estimate the unmeasured linear velocity and disturbances, the control system proposed in this paper gives more desirable information (an

exponential estimate of linear velocity and disturbances) and does not need to introduce a leakage term or to use a projection algorithm to prevent a parameter drift problem.

The rest of the paper is organized as follows. In Section 2., the aircraft's equations of motion and control objectives are presented. The one-step ahead backstepping method is introduced in Section 3.. The control design is presented in Section 4.. Exponential observers for estimating the linear velocity and disturbances are given in Section 5.. Section 6. gives numerical simulation results. Proofs of the results are given in Appendices A, B, and C.

2. PROBLEM STATEMENT

2.1. Aircraft dynamics

Under the assumption that the aerodynamics are neglected, the Lagrangian approach results in the following equations of motion of the quadrotor aircraft (see [**?**]):

$$\begin{cases} \dot{\boldsymbol{\eta}}_1 = \boldsymbol{v}_1, \\ \dot{\boldsymbol{v}}_1 = -g\boldsymbol{e}_3 + \frac{1}{m} f \boldsymbol{R}_1(\boldsymbol{q})\boldsymbol{e}_3, \end{cases} \quad \begin{cases} \dot{\boldsymbol{q}} = \boldsymbol{K}(\boldsymbol{q})\boldsymbol{\omega}, \\ \dot{\boldsymbol{\omega}} = -\boldsymbol{J}^{-1}\boldsymbol{S}(\boldsymbol{\omega})\boldsymbol{J}\boldsymbol{\omega} + \boldsymbol{J}^{-1}\boldsymbol{\tau}, \end{cases} \tag{1}$$

where $\boldsymbol{e}_3 = [0\ 0\ 1]^T$, g is the gravity acceleration, m is the mass of the aircraft, $\boldsymbol{J}$ is the inertia matrix of the aircraft. The vector $\boldsymbol{\eta}_1 = [x\ y\ z]^T$ denotes the (surge, sway, heave) displacements of the center of mass of the aircraft coordinated in the earth-fixed frame. The vector $\boldsymbol{v}_1 = [u\ v\ w]^T$ denotes the (surge, sway, heave) velocities of the aircraft coordinated in the earth-fixed frame. The skew-symmetric matrix $\boldsymbol{S}(\boldsymbol{x})$ is defined as $\boldsymbol{S}(\boldsymbol{x})\boldsymbol{y} = \boldsymbol{x} \times \boldsymbol{y}$ for all $\boldsymbol{y} \in \mathbb{R}^3$, where $'\times'$ denotes the vector cross product. The unit-quaternion $\boldsymbol{q} = [q_0\ \bar{\boldsymbol{q}}^T]^T$, which represents the attitude (orientation) of the aircraft coordinated in the body-fixed frame, is a four-element vector composed of a scalar component q_0 and a vector component $\bar{\boldsymbol{q}} \in \mathbb{R}^3$ that satisfy $q_0^2 + \|\bar{\boldsymbol{q}}\|^2 = 1$. The vector $\boldsymbol{\omega}$ denotes the aircraft's angular velocity vector coordinated in the body-fixed frame. The matrices $\boldsymbol{R}_1(\boldsymbol{q})$ and $\boldsymbol{K}(\boldsymbol{q})$ are given by

$$\boldsymbol{R}_1(\boldsymbol{q}) = (q_0^2 - \|\bar{\boldsymbol{q}}\|^2)\boldsymbol{I}_{3\times 3} + 2\bar{\boldsymbol{q}}\bar{\boldsymbol{q}}^T + 2q_0\boldsymbol{S}(\bar{\boldsymbol{q}}), \quad \boldsymbol{K}(\boldsymbol{q}) = \frac{1}{2}\begin{bmatrix} -\bar{\boldsymbol{q}}^T \\ q_0\boldsymbol{I}_{3\times 3} + \boldsymbol{S}(\bar{\boldsymbol{q}}) \end{bmatrix}, \tag{2}$$

where $\boldsymbol{I}_{3\times 3}$ is the 3×3 identity matrix. Note that $\boldsymbol{K}^T(\boldsymbol{q})\boldsymbol{K}(\boldsymbol{q}) = \frac{1}{4}\boldsymbol{I}_{3\times 3}$. The force f and the moment vector $\boldsymbol{\tau}$ are given by

$$f = \sum_{i=1}^{4} f_i, \quad \boldsymbol{\tau} = \begin{bmatrix} (f_4 - f_2)L \\ (f_3 - f_1)L \\ (f_2 - f_1 + f_4 - f_3)C_a \end{bmatrix}, \tag{3}$$

where $f_i, i = 1, .., 4$ is the thrust generated by the i^{th} rotor along the i^{th} rotor axis, L is the distance between the rotor and the aircraft's center of mass, and C_a is a coefficient relating the difference in the rotor's speed to the yaw moment about the vertical body axis. The aircraft dynamics (1) is underactuated if we are interested in controlling all six outputs (surge, sway, heave, roll, pitch and yaw) since there are only four independent control inputs $f_i, i = 1, \cdots, 4$.

For the purpose of the control design later, we let ϕ, θ, and ψ be the roll, pitch, and yaw angles, respectively, coordinated in the body-fixed frame. The unit-quaternion $\boldsymbol{q}$ can be given in terms of ϕ, θ, and ψ as follows, see [**?**]:

$$\boldsymbol{q}(\boldsymbol{\eta}_2) = \begin{bmatrix} \cos(\frac{\phi}{2})\cos(\frac{\theta}{2})\cos(\frac{\psi}{2}) + \sin(\frac{\phi}{2})\sin(\frac{\theta}{2})\sin(\frac{\psi}{2}) \\ \sin(\frac{\phi}{2})\cos(\frac{\theta}{2})\cos(\frac{\psi}{2}) - \cos(\frac{\phi}{2})\sin(\frac{\theta}{2})\sin(\frac{\psi}{2}) \\ \cos(\frac{\phi}{2})\sin(\frac{\theta}{2})\cos(\frac{\psi}{2}) + \sin(\frac{\phi}{2})\cos(\frac{\theta}{2})\sin(\frac{\psi}{2}) \\ \cos(\frac{\phi}{2})\cos(\frac{\theta}{2})\sin(\frac{\psi}{2}) - \sin(\frac{\phi}{2})\sin(\frac{\theta}{2})\cos(\frac{\psi}{2}) \end{bmatrix}, \tag{4}$$

with $\boldsymbol{\eta}_2 = [\phi\ \theta\ \psi]^T$. Using (4), we can write the matrix $\boldsymbol{R}_1(\boldsymbol{q}) = \boldsymbol{R}_1(\boldsymbol{\eta}_2)$ defined in (2) as

$$\boldsymbol{R}_1(\boldsymbol{\eta}_2) = \begin{bmatrix} \cos(\psi)\cos(\theta) & -\sin(\psi)\cos(\phi) + \sin(\phi)\sin(\theta)\cos(\psi) & \sin(\psi)\sin(\phi) + \sin(\theta)\cos(\psi)\cos(\phi) \\ \sin(\psi)\cos(\theta) & \cos(\psi)\cos(\phi) + \sin(\phi)\sin(\theta)\sin(\psi) & -\cos(\psi)\sin(\phi) + \sin(\theta)\sin(\psi)\cos(\phi) \\ -\sin(\theta) & \sin(\phi)\cos(\theta) & \cos(\phi)\cos(\theta) \end{bmatrix}.$$

2.2. Control objective

Control Objective 2..1 *Assume that the reference position trajectory* $\boldsymbol{\eta}_{1d}(t) = [x_d(t)\ y_d(t)\ z_d(t)]^T$ *is sufficiently smooth, i.e., its first four derivatives exist and are bounded in the sense that there exist non-negative constants* ϱ_1, ϱ_2,

ϱ_3, ϱ_4 such that

$$\sup_{t\in\mathbb{R}^+}\|\dot{\boldsymbol{\eta}}_{1d}(t)\|\leq\varrho_1,\ \sup_{t\in\mathbb{R}^+}\|\ddot{\boldsymbol{\eta}}_{1d}(t)\|\leq\varrho_2,\ \sup_{t\in\mathbb{R}^+}\|\dddot{\boldsymbol{\eta}}_{1d}(t)\|\leq\varrho_3,\ \sup_{t\in\mathbb{R}^+}\|\ddddot{\boldsymbol{\eta}}_{1d}(t)\|\leq\varrho_4. \tag{5}$$

Moreover, the absolute value of the second derivative of $z_{1d}(t)$ is assumed to be strictly less than g, i.e.,

$$\sup_{t\in\mathbb{R}^+}|\ddot{z}_{1d}(t)|\leq g-\varrho_5, \tag{6}$$

where ϱ_5 is a strictly positive constant. The reference yaw angle $\psi_d(t)$ is also assumed to be sufficiently smooth in the sense that its first two derivatives exist and are bounded, i.e., there exist non-negative constants ϱ_6 and ϱ_7 such that

$$\sup_{t\in\mathbb{R}^+}|\dot{\psi}_{1d}(t)|\leq\varrho_6,\ \sup_{t\in\mathbb{R}^+}|\ddot{\psi}_{1d}(t)|\leq\varrho_7. \tag{7}$$

Under the above assumptions, design the control inputs f_i, $i=1,\cdots,4$ such that the position vector $\boldsymbol{\eta}_1(t)$ and the yaw angle $\psi(t)$ of the aircraft globally asymptotically and locally exponentially track their reference trajectories $\boldsymbol{\eta}_{1d}(t)$ and $\psi_d(t)$, i.e.,

$$\lim_{t\to\infty}(\boldsymbol{\eta}_1(t)-\boldsymbol{\eta}_{1d}(t))=0,\quad \lim_{t\to\infty}(\psi(t)-\psi_d(t))=0, \tag{8}$$

while keep all other states of the aircraft dynamics bounded for all initial conditions $\boldsymbol{\eta}_1(t_0)\in\mathbb{R}^3$, $\boldsymbol{v}_1(t_0)\in\mathbb{R}^3$, $\boldsymbol{q}(t_0)\in\mathbb{R}^3$ with $\|\boldsymbol{q}(t_0)\|^2=1$, and $\boldsymbol{\omega}(t_0)\in\mathbb{R}^3$.

Remark 2..1 *The condition (6) implies that the aircraft is not allowed to land faster than it freely falls under the gravitational force. We need this condition to design a continuous and global trajectory tracking controller.*

3. PRELIMINARIES

In this section, we present a smooth saturation function and a one-step ahead backstepping method, which will be used in the control design and stability analysis in the next section.

3.1. Smooth saturation function

Definition 3..1 *The function $\sigma(x)$ is said to be a smooth saturation function if it possesses the following properties:*

$$\begin{aligned}&\sigma(0)=0,\ \sigma(x)x>0,\ \forall\ x\in\{\mathbb{R}-0\},\\&(x-y)[\sigma(x)-\sigma(y)]\geq 0,\ \forall\ (x,y)\in\mathbb{R}^2,\\&\sigma(-x)=-\sigma(x),\ |\sigma(x)|\leq 1,\ \frac{\sigma(x)}{x}\leq 1,\ 0<\frac{d\sigma(x)}{dx}\leq 1,\ \forall\ x\in\mathbb{R}.\end{aligned}$$

Some functions satisfying the above properties include $\sigma(x)=\tanh(x)$ and $\sigma(x)=\frac{x}{\sqrt{1+x^2}}$. For the vector $\boldsymbol{x}=[x_1,\cdots,x_i,\cdots,x_n]^T$, we use the notation $\boldsymbol{\sigma}(\boldsymbol{x})=[\sigma(x_1),\cdots,\sigma(x_i),\cdots,\sigma(x_n)]^T$ to denote the smooth saturation function vector of $\boldsymbol{x}$.

3.2. One step ahead backstepping method

Consider the following second-order system:

$$\begin{aligned}\dot{x}_1&=x_2+f_1(t,x_1,x_2),\\\dot{x}_2&=u+f_2(t,x_1,x_2),\end{aligned} \tag{9}$$

where t denotes time, x_1 and x_2 are the states, u is the control input, and we assume that

$$|f_1(\bullet)|\leq\varrho_{11},\ \left|\frac{\partial f_1(\bullet)}{\partial t}\right|\leq\varrho_{12},\ \left|\frac{\partial f_1(\bullet)}{\partial x_2}\right|\leq\varrho_{13},\ \left|\frac{\partial f_1(\bullet)}{\partial x_1}x_2\right|\leq\varrho_{14},\ \left|\frac{\partial f_1(\bullet)}{\partial x_1}\right|\leq\varrho_{15},\ |f_2(\bullet)|\leq\varrho_{21}, \tag{10}$$

for all $t\in\mathbb{R}^+$, and $(x_1,x_2)\in\mathbb{R}^2$. In (10), $\bullet$ stands for (t,x_1,x_2), and ϱ_{1i}, $i=1,...,5$, and ϱ_{21} are nonnegative constants with ϱ_{13} strictly less than 1. It is noted that we need to impose the conditions (10) on $f_1(t,x_1,x_2)$ and

$f_2(t,x_1,x_2)$ to make it possible to design a bounded control u that can globally and asymptotically and locally exponentially stabilize (9) at the origin. For example if $f_2(t,x_1,x_2)$ is not bounded by a constant, we cannot design a bounded control u to globally and asymptotically and locally exponentially stabilize (9) at the origin since the control u needs to cancel the term $f_2(t,x_1,x_2)$ in general.

Let us address the problem of designing u to globally and asymptotically and locally exponentially stabilize (9) at the origin such that $|u(t)|$ is bounded for all $t \geq t_0 \geq 0$ by a positive constant for all $(x_1(t_0), x_2(t_0)) \in \mathbb{R}^2$ at the initial time $t_0 \geq 0$. The one-step ahead backstepping control design consists of two steps.

Step 1. Define $x_{2e} = x_2 - \alpha_1$, where α_1 is the virtual control of x_2. Let us consider the Lyapunov function candidate

$$V_1 = \int_0^{x_1} \sigma(s)ds, \tag{11}$$

where $\sigma(s)$ is a smooth saturation function defined in Definition 3..1. By differentiating both sides of (11), we choose the virtual control α_1 as

$$\alpha_1 = \frac{-k_1\sigma(x_1)}{\Delta_1(x_2)} - f_1(t,x_1,x_2), \tag{12}$$

where k_1 is a positive constant such that $k_1+\varrho_{13}$ is less than 1, and the function $\Delta_1(x_2)$ is chosen as $\Delta_1(x_2) = 1+\frac{1}{2}x_2^2$. Now substituting (12) and $x_{2e} = x_2 - \alpha_1$ into the derivative of V_1 results in $\dot{V}_1 = \frac{-k_1\sigma(x_1)^2}{\Delta_1(x_2)} + \sigma(x_1)x_{2e}$.

Step 2. Consider the Lyapunov function

$$V_2 = \gamma V_1 + \frac{1}{2}x_{2e}^2, \tag{13}$$

where γ is a positive constant. With $x_{2e} = x_2 - \alpha_1$ and $\dot{V}_1 = \frac{-k_1\sigma(x_1)^2}{\Delta_1(x_2)} + \sigma(x_1)x_{2e}$, where α_1 is given in (12), differentiating both sides of (13) and choosing the actual control u as

$$u = \left(1 - \frac{\partial\alpha_1}{\partial x_2}\right)^{-1}\left(-k_2\sigma(x_{2e}) - \gamma\sigma(x_1) + \frac{\partial\alpha_1}{\partial t} + \frac{\partial\alpha_1}{\partial x_1}\Big(x_2 + f_1(t,x_1,x_2)\Big)\right) - f_2(t,x_1,x_2) \tag{14}$$

result in

$$\dot{V}_2 = \frac{-k_1\gamma\sigma(x_1)^2}{\Delta_1(x_2)} - k_2\sigma(x_{2e})x_{2e}. \tag{15}$$

Since $\left|\frac{\partial\alpha_1}{\partial x_2}\right| \leq k_1 + \varrho_{13}$ for all $(x_1,x_2) \in \mathbb{R}^2$ and $k_1 + \varrho_{13} < 1$, the control u given in (14) is well defined. Based on (11), (13) and (15), it is readily shown that the closed loop system consisting of (9) and (14) is forward complete and is globally asymptotically and locally exponentially stable at the origin. From (14) a calculation shows that

$$|u(t)| \leq \frac{k_2 + \gamma + \varrho_{12} + k_1 + \varrho_{14} + (k_1 + \varrho_{15})\varrho_{11}}{1 - k_1 - \varrho_{13}} + \varrho_{21}, \tag{16}$$

for all $t \geq t_0 \geq 0$. The above bound means that the magnitude of the control input u is bounded by a positive constant for all initial conditions $x_1(t_0) \in \mathbb{R}$ and $x_2(t_0) \in \mathbb{R}$.

Remark 3..1

1. *The main difference between the above control design and the standard backstepping method [?] is that the virtual control α_1 in (12) is a function of both x_1 and x_2. This is crucial to allow us to design the bounded control u in (14), see the term $\frac{\partial\alpha_1}{\partial x_1}x_2$.*

2. *There are several other methods (e.g., [?], [?]) to design bounded control laws for a chain of integrators inspired by the work in [?]. However, it is difficult to apply these methods for designing global tracking controllers for the quadrotor aircraft in this paper.*

3. *Although the one-step ahead backstepping method has been presented for a second-order system, it can be straightforwardly to extend to a higher order system.*

4. CONTROL DESIGN

For clarity, the control design is presented for the quadrotor aircraft with full-state available for feedback and without disturbances. The problem with disturbances and without linear velocity measurement is readily solved by combining the control design proposed in this section and exponential observers for estimating the linear velocity vector $\boldsymbol{v}_1$ and disturbances in Section 5.. The control design consists of two stages. In the first stage, the first two equations of (1) will be considered. Using the one-step ahead backstepping method introduced in Subsection 3.2. we will design the total thrust f and the virtual controls of the roll and pitch angles to globally asymptotically stabilize the tracking error vector $\boldsymbol{\eta}_1(t) - \boldsymbol{\eta}_{1d}(t)$ at the origin. In the second stage, the last two equations of (1) will be considered. Using the backstepping technique [?], the moment vector $\boldsymbol{\tau}$ will be designed to globally asymptotically and locally exponentially stabilize the tracking error $\psi(t) - \psi_d(t)$ and the errors between the virtual controls of the roll and pitch angles and their actual values at the origin.

4.1. Stage 1

This stage consists of two steps.

4.1.1. Step 1

In this step, the first equation of (1) is considered. We will design a virtual control of $\boldsymbol{v}_1$ to force $\boldsymbol{\eta}_1(t)$ to globally asymptotically and locally exponentially track its reference trajectory $\boldsymbol{\eta}_{1d}(t)$. As such, we define

$$\begin{aligned} \boldsymbol{\eta}_{1e} &= \boldsymbol{\eta}_1 - \boldsymbol{\eta}_{1d}, \\ \boldsymbol{v}_{1e} &= \boldsymbol{v}_1 - \boldsymbol{\alpha}_{\boldsymbol{v}_1}, \end{aligned} \tag{17}$$

where $\boldsymbol{\alpha}_{\boldsymbol{v}_1}$ is a virtual control of $\boldsymbol{v}_1$. Substituting (17) into the first equation of (1) results in

$$\dot{\boldsymbol{\eta}}_{1e} = \boldsymbol{\alpha}_{\boldsymbol{v}_1} + \boldsymbol{v}_{1e} - \dot{\boldsymbol{\eta}}_{1d}. \tag{18}$$

To design the virtual control $\boldsymbol{\alpha}_{\boldsymbol{v}_1}$, we consider the Lyapunov function candidate

$$V_1 = \int_0^{\boldsymbol{\eta}_{1e}} \boldsymbol{\sigma}^T(\boldsymbol{s})d\boldsymbol{s}, \tag{19}$$

whose derivative along the solutions of (18) satisfies

$$\dot{V}_1 = \boldsymbol{\sigma}^T(\boldsymbol{\eta}_{1e})(\boldsymbol{\alpha}_{\boldsymbol{v}_1} + \boldsymbol{v}_{1e} - \dot{\boldsymbol{\eta}}_{1d}), \tag{20}$$

which suggests that we use the one-step ahead backstepping method introduced in Subsection 3.2. to design the virtual control $\boldsymbol{\alpha}_{\boldsymbol{v}_1}$ as follows

$$\boldsymbol{\alpha}_{\boldsymbol{v}_1} = -\boldsymbol{K}_1 \frac{\boldsymbol{\sigma}(\boldsymbol{\eta}_{1e})}{\Delta(\boldsymbol{v}_1)} + \dot{\boldsymbol{\eta}}_{1d}, \tag{21}$$

where $\boldsymbol{K}_1 = \text{diag}(k_{11}, k_{12}, k_{13})$ with k_{11}, k_{12}, and k_{13} being positive constants to be chosen later. The term $\Delta(\boldsymbol{v}_1)$ is chosen as

$$\Delta(\boldsymbol{v}_1) = 1 + \frac{1}{2}\|\boldsymbol{v}_1\|^2. \tag{22}$$

Substituting (21) into (20) gives

$$\dot{V}_1 = -\frac{\boldsymbol{\sigma}^T(\boldsymbol{\eta}_{1e})\boldsymbol{K}_1\boldsymbol{\sigma}(\boldsymbol{\eta}_{1e})}{\Delta(\boldsymbol{v}_1)} + \boldsymbol{\sigma}^T(\boldsymbol{\eta}_{1e})\boldsymbol{v}_{1e}. \tag{23}$$

On the other hand, substituting (21) into (18) yields

$$\dot{\boldsymbol{\eta}}_{1e} = -\boldsymbol{K}_1 \frac{\boldsymbol{\sigma}(\boldsymbol{\eta}_{1e})}{\Delta(\boldsymbol{v}_1)} + \boldsymbol{v}_{1e}. \tag{24}$$

To prepare for the next step, we calculate $\dot{\boldsymbol{v}}_{1e}$ by differentiating both side of the second equation of (17) along the solutions of (21) and the second equation of (1) to obtain

$$\dot{\boldsymbol{v}}_{1e} = \boldsymbol{G}_1\Big(- g\boldsymbol{e}_3 + \frac{1}{m} f \boldsymbol{R}_1(\boldsymbol{q})\boldsymbol{e}_3\Big) + \boldsymbol{F}_1 - \ddot{\boldsymbol{\eta}}_{1d}, \tag{25}$$

where

$$\boldsymbol{G}_1 = \boldsymbol{I}_{3\times 3} - \boldsymbol{K}_1 \frac{\boldsymbol{\sigma}(\boldsymbol{\eta}_{1e})\boldsymbol{v}_1^T}{\Delta^2(\boldsymbol{v}_1)},$$
$$\boldsymbol{F}_1 = \boldsymbol{K}_1 \frac{\boldsymbol{\sigma}'(\boldsymbol{\eta}_{1e})}{\Delta(\boldsymbol{v}_1)}\Big(- \boldsymbol{K}_1 \frac{\boldsymbol{\sigma}(\boldsymbol{\eta}_{1e})}{\Delta(\boldsymbol{v}_1)} + \boldsymbol{v}_{1e}\Big), \quad \boldsymbol{\sigma}'(\boldsymbol{\eta}_{1e}) = \frac{\partial \boldsymbol{\sigma}(\boldsymbol{\eta}_{1e})}{\partial \boldsymbol{\eta}_{1e}}. \tag{26}$$

Let $\boldsymbol{v}_1$ and $\boldsymbol{\sigma}(\boldsymbol{\eta}_{1e})$ be written in their components as $\boldsymbol{v}_1 = [v_{11}\ v_{12}\ v_{13}]^T$ and $\boldsymbol{\sigma}(\boldsymbol{\eta}_{1e}) = [\sigma(\eta_{11e})\ \sigma(\eta_{12e})\ \sigma(\eta_{13e})]^T$. From (26), we calculate the determinant of $\boldsymbol{G}_1$ as follows:

$$\det(\boldsymbol{G}_1) = 1 - k_{11}\frac{\sigma(\eta_{11e})v_{11}}{\Delta^2(\boldsymbol{v}_1)} - k_{12}\frac{\sigma(\eta_{12e})v_{12}}{\Delta^2(\boldsymbol{v}_1)} - k_{13}\frac{\sigma(\eta_{13e})v_{13}}{\Delta^2(\boldsymbol{v}_1)} \geq 1 - \frac{\sqrt{2}}{2}(k_{11}+k_{12}+k_{13}). \tag{27}$$

Therefore, we choose the elements k_{11}, k_{12}, and k_{13} of the matrix such that

$$1 - \frac{\sqrt{2}}{2}(k_{11}+k_{12}+k_{13}) > 0 \tag{28}$$

to ensure that the matrix $\boldsymbol{G}_1$ is invertible. Moreover, substituting $\boldsymbol{v}_{1e}$ defined in the second equation of (17) with $\boldsymbol{\alpha}_1(\boldsymbol{v}_1)$ defined in (21) into the expression of the the vector $\boldsymbol{F}_1$ defined in the second equation of (26) gives

$$\boldsymbol{F}_1 = \boldsymbol{K}_1 \frac{\boldsymbol{\sigma}'(\boldsymbol{\eta}_{1e})}{\Delta(\boldsymbol{v}_1)}\big(\boldsymbol{v}_1 - \dot{\boldsymbol{\eta}}_{1d}\big). \tag{29}$$

Using the expression of $\Delta(\boldsymbol{v}_1)$ defined in (22), we have the following bound of $\boldsymbol{F}_1$:

$$\|\boldsymbol{F}_1\| \leq \lambda_M(\boldsymbol{K}_1)\Big(2 + \varrho_1\Big), \tag{30}$$

where ϱ_1 is defined in (5), and $\lambda_M(\boldsymbol{K}_1)$ is the maximum eigenvalue of $\boldsymbol{K}_1$.

4.1.2. Step 2

We define

$$\boldsymbol{q}_e = \boldsymbol{q} \pm \boldsymbol{\alpha}_{\boldsymbol{q}} \tag{31}$$

where $\boldsymbol{\alpha}_{\boldsymbol{q}} = [\alpha_{q_0}\ \boldsymbol{\alpha}_{\bar{\boldsymbol{q}}}^T]^T$ with $\boldsymbol{\alpha}_{\bar{\boldsymbol{q}}} = [\alpha_{q_1}\ \alpha_{q_2}\ \alpha_{q_3}]^T$ is a virtual control of $\boldsymbol{q}$. We use the $\pm$ in (31) to resolve the sign ambiguity since $\boldsymbol{q} = [q_0\ \bar{\boldsymbol{q}}^T]^T$ must satisfy the constraint $q_0^2 + \|\bar{\boldsymbol{q}}\|^2 = 1$. The $\pm$ sign in (31) results in the same desired orientation of the aircraft when $\boldsymbol{q}_e$ is equal to zero. This is because from (4) we have $\boldsymbol{q}(\boldsymbol{\eta}_2) = -\boldsymbol{q}(\boldsymbol{\eta}_2 \pm 2\pi)$. Therefore, $\boldsymbol{\alpha}_{\boldsymbol{q}}$ represents the desired Euler angles corresponding to those, which are represented by $-\boldsymbol{\alpha}_{\boldsymbol{q}}$, rotated by an angle of 2π. Substituting (31) into (2) results in

$$\boldsymbol{R}_1(\boldsymbol{q}) = \boldsymbol{R}_1(\boldsymbol{\alpha}_{\boldsymbol{q}}) + \boldsymbol{H}(\boldsymbol{q}_e, \boldsymbol{\alpha}_{\boldsymbol{q}}), \tag{32}$$

where

$$\boldsymbol{H}(\boldsymbol{q}_e, \boldsymbol{\alpha}_{\boldsymbol{q}}) = \Big[q_{0e}(q_{0e} \pm 2\alpha_{q_0}) - \bar{\boldsymbol{q}}_e^T(\bar{\boldsymbol{q}}_e \pm 2\boldsymbol{\alpha}_{\bar{\boldsymbol{q}}})\Big]\boldsymbol{I}_{3\times 3} + 2\bar{\boldsymbol{q}}_e(\bar{\boldsymbol{q}}_e^T \pm 2\boldsymbol{\alpha}_{\bar{\boldsymbol{q}}}^T) + 2\Big[q_{0e}(\boldsymbol{S}(\bar{\boldsymbol{q}}_e)) \pm \boldsymbol{S}(\boldsymbol{\alpha}_{\bar{\boldsymbol{q}}}) \pm \alpha_{q_0}\boldsymbol{S}(\bar{\boldsymbol{q}}_e)\Big], \tag{33}$$

since $\boldsymbol{S}(\boldsymbol{x}+\boldsymbol{y}) = \boldsymbol{S}(\boldsymbol{x}) + \boldsymbol{S}(\boldsymbol{y})$ for all $\boldsymbol{x} \in \mathbb{R}^3$ and $\boldsymbol{y} \in \mathbb{R}^3$. Now let us define $\boldsymbol{\alpha}_{\boldsymbol{\eta}_2} = [\alpha_\phi\ \alpha_\theta\ \alpha_\psi]^T$ with

$$\alpha_\psi = \psi_d, \tag{34}$$

which is the virtual control of $\boldsymbol{\eta}_2$ corresponding to the virtual unit-quaternion vector $\boldsymbol{\alpha}_{\boldsymbol{q}}$. Using (5), we can write $\boldsymbol{R}_1(\boldsymbol{\alpha}_{\boldsymbol{q}}) = \boldsymbol{R}_1(\boldsymbol{\alpha}_{\boldsymbol{\eta}_2})$ as

$$\boldsymbol{R}_1(\boldsymbol{\alpha}_{\boldsymbol{q}}) = \boldsymbol{R}_1(\boldsymbol{\eta}_2)\big|_{\boldsymbol{\eta}_2 = \boldsymbol{\alpha}_{\boldsymbol{\eta}_2}}, \tag{35}$$

where using (4) we have the relationship between $\boldsymbol{\alpha}_{\boldsymbol{q}}$ and $\boldsymbol{\alpha}_{\boldsymbol{\eta}_2}$ as follows:

$$\boldsymbol{\alpha}_{\boldsymbol{q}} = \boldsymbol{q}(\boldsymbol{\eta}_2)\big|_{\boldsymbol{\eta}_2 = \boldsymbol{\alpha}_{\boldsymbol{\eta}_2}}. \tag{36}$$

The purpose of writing down (35) and (36) is that it is difficult to design the virtual control $\boldsymbol{\alpha}_{\boldsymbol{q}}$ to globally asymptotically stabilize the error vector $\boldsymbol{v}_{1e}$ at the origin. Therefore, we will design the virtual control $\boldsymbol{\alpha}_{\boldsymbol{\eta}_2}$ (only α_ϕ and α_θ

since α_ψ is already available in (34)) by using (35) then the virtual control $\boldsymbol{\alpha_q}$ will be found by substituting $\boldsymbol{\alpha_{\eta_2}}$ into (36). To design the control f and the virtual control $\boldsymbol{\alpha_{\eta_2}}$, we consider the Lyapunov function candidate

$$V_2 = \gamma V_1 + \frac{1}{2}\|\boldsymbol{v}_{1e}\|^2, \tag{37}$$

where γ is a positive constant. Differentiating both sides of (37) along the solutions of (23), (25), and (32) gives

$$\dot{V}_2 = -\gamma\frac{\boldsymbol{\sigma}^T(\boldsymbol{\eta}_{1e})\boldsymbol{K}_1\boldsymbol{\sigma}(\boldsymbol{\eta}_{1e})}{\Delta(\boldsymbol{v}_1)} + \boldsymbol{v}_{1e}^T\Big[\gamma\boldsymbol{\sigma}(\boldsymbol{\eta}_{1e}) + \boldsymbol{G}_1\Big(-g\boldsymbol{e}_3 + \frac{1}{m}f\boldsymbol{R}_1(\boldsymbol{\alpha_q})\boldsymbol{e}_3\Big) + \boldsymbol{F}_1 - \ddot{\boldsymbol{\eta}}_{1d}\Big] + \boldsymbol{v}_{1e}^T\boldsymbol{G}_1\frac{1}{m}f\boldsymbol{H}(\boldsymbol{q}_e, \boldsymbol{\alpha_q})\boldsymbol{e}_3, \tag{38}$$

which suggests that we choose

$$f\boldsymbol{R}_1(\boldsymbol{\alpha_q})\boldsymbol{e}_3 = m\boldsymbol{G}_1^{-1}\big(-\boldsymbol{K}_2\boldsymbol{\sigma}(\boldsymbol{v}_{1e}) - \boldsymbol{F}_1 - \gamma\boldsymbol{\sigma}(\boldsymbol{\eta}_{1e}) + \ddot{\boldsymbol{\eta}}_{1d}\big) + mg\boldsymbol{e}_3 \triangleq \boldsymbol{\Omega}, \tag{39}$$

where $\boldsymbol{K}_2 = \mathrm{diag}(k_{21}, k_{22}, k_{23})$ with k_{21}, k_{22}, and k_{23} positive constants to be chosen later. Let Ω_1, Ω_2, and Ω_3 be the elements of $\boldsymbol{\Omega}$, i.e., $\boldsymbol{\Omega} = [\Omega_1\ \Omega_2\ \Omega_3]^T$. From (39), we obtain the upper bounds of $|\Omega_1|$, $|\Omega_2|$, and $|\Omega_3|$, and lower-bound of Ω_3:

$$\begin{aligned}
|\Omega_1| \le& \frac{m}{\varrho_0}\Big((1-k_{12}-k_{13})(k_{21}+\lambda_M(\boldsymbol{K}_1)(2+\varrho_1)+\gamma+\varrho_{21}) + k_{11}(2k_{13}+1)\times \\
&(k_{22}+\lambda_M(\boldsymbol{K}_1)(2+\varrho_1)+\gamma+\varrho_{22}) + k_{11}(2k_{12}+1)(k_{23}+\lambda_M(\boldsymbol{K}_1)(2+\varrho_1)+\gamma+\varrho_{23})\Big) := \Omega_{1M}, \\
|\Omega_2| \le& \frac{m}{\varrho_0}\Big(k_{12}(2k_{13}+1)(k_{21}+\lambda_M(\boldsymbol{K}_1)(1+0.5\varrho_1)+\gamma+\varrho_{21}) + (1-k_{11}-k_{13})\times \\
&(k_{22}+\lambda_M(\boldsymbol{K}_1)(2+\varrho_1)+\gamma+\varrho_{22}) + k_{12}(2k_{11}+1)(k_{23}+\lambda_M(\boldsymbol{K}_1)(2+\varrho_1)+\gamma+\varrho_{23})\Big) := \Omega_{2M}, \\
|\Omega_3| \le& \frac{m}{\varrho_0}\Big(k_{13}(2k_{12}+1)(k_{21}+\lambda_M(\boldsymbol{K}_1)(2+\varrho_1)+\gamma+\varrho_{21}) + k_{13}(2k_{11}+1)(k_{22}+\lambda_M(\boldsymbol{K}_1)\times \\
&(2+\varrho_1)+\gamma+\varrho_{22}) + (1-k_{11}-k_{12})(k_{23}+\lambda_M(\boldsymbol{K}_1)(2+\varrho_1)+\gamma+\varrho_{23})\Big) + mg := \Omega_{3M}, \\
\Omega_3 \ge& -\frac{m}{\varrho_0}\Big(k_{13}(2k_{12}+1)(k_{21}+\lambda_M(\boldsymbol{K}_1)(2+\varrho_1)+\gamma+\varrho_{21}) + k_{13}(2k_{11}+1)\times \\
&(k_{22}+\lambda_M(\boldsymbol{K}_1)(2+\varrho_1)+\gamma+\varrho_{22}) + (1-k_{11}-k_{12})(k_{23}+\lambda_M(\boldsymbol{K}_1)(2+\varrho_1)+\gamma+\varrho_{23})\Big) + mg,
\end{aligned} \tag{40}$$

where $\varrho_0 = 1 - \frac{\sqrt{2}}{2}(k_{11}+k_{12}+k_{13})$, $\varrho_{21} = \sup_{t\in\mathbb{R}^+}|\ddot{x}_{1d}(t)|$, $\varrho_{22} = \sup_{t\in\mathbb{R}^+}|\ddot{y}_{1d}(t)|$, and $\varrho_{23} = \sup_{t\in\mathbb{R}^+}|\ddot{z}_{1d}(t)|$. We now specify the gain matrices and the constant γ such that $\Omega_3 \ge \Omega_3^*$ with Ω_3^* being a strictly positive constant, i.e.,

$$\begin{aligned}
\Omega_3 \ge& \frac{-m}{\varrho_0}\Big(k_{13}(2k_{12}+1)(k_{21}+\lambda_M(\boldsymbol{K}_1)(2+\varrho_1)+\gamma+\varrho_{21}) + k_{13}(2k_{11}+1)(k_{22}+\lambda_M(\boldsymbol{K}_1)\times \\
&(2+\varrho_1)+\gamma+\varrho_{22}) + (1-k_{11}-k_{12})(k_{23}+\lambda_M(\boldsymbol{K}_1)(2+\varrho_1)+\gamma+g-\varrho_5)\Big) + mg \ge \Omega_3^*,
\end{aligned} \tag{41}$$

where we have used (6). Since ϱ_5 is a strictly positive constant, we can choose sufficiently small $\boldsymbol{K}_1$, $\boldsymbol{K}_2$, and γ such that the condition (41) holds. This condition is necessary for designing a global control law for α_θ later. As such, the equation (39) yields $f\boldsymbol{e}_3 = \boldsymbol{R}_1^{-1}(\boldsymbol{\alpha_q})\boldsymbol{\Omega}$. Since $\boldsymbol{R}_1^{-T}(\boldsymbol{\alpha_q})\boldsymbol{R}_1^{-1}(\boldsymbol{\alpha_q}) = \boldsymbol{I}_{3\times3}$, we have

$$f = \sqrt{\boldsymbol{\Omega}^T\boldsymbol{\Omega}}. \tag{42}$$

Since $\Omega \ge \Omega_3^*$, see (41), we have $f = \sqrt{\Omega_1^2+\Omega_2^2+\Omega_3^2} \ge \Omega_3^*$. On the other hand, we expand the term $\boldsymbol{R}_1^{-1}(\boldsymbol{\alpha_q})\boldsymbol{\Omega}$ using (35) and $\boldsymbol{e}_3 = [0\ 0\ 1]^T$ to obtain

$$\begin{aligned}
&\cos(\alpha_\psi)\cos(\alpha_\theta)\Omega_1 + \sin(\alpha_\psi)\cos(\alpha_\theta)\Omega_2 - \sin(\alpha_\theta)\Omega_3 = 0, \\
&\big[-\sin(\alpha_\psi)\cos(\alpha_\phi) + \sin(\alpha_\phi)\sin(\alpha_\theta)\cos(\alpha_\psi)\big]\Omega_1 + \big[\cos(\alpha_\psi)\cos(\alpha_\phi) + \sin(\alpha_\phi)\sin(\alpha_\theta)\sin(\alpha_\psi)\big]\Omega_2 + \\
&\qquad \sin(\alpha_\phi)\cos(\alpha_\theta)\Omega_3 = 0, \\
&\big[\sin(\alpha_\psi)\sin(\alpha_\phi) + \sin(\alpha_\theta)\cos(\alpha_\psi)\cos(\alpha_\phi)\big]\Omega_1 + \big[-\cos(\alpha_\psi)\sin(\alpha_\phi) + \sin(\alpha_\theta)\sin(\alpha_\psi)\cos(\alpha_\phi)\big]\Omega_2 + \\
&\qquad \cos(\alpha_\phi)\cos(\alpha_\theta)\Omega_3 = f.
\end{aligned} \tag{43}$$

Now multiplying the second equation of (43) by $-\cos(\alpha_\phi)$ then adding with the third equation of (43) multiplied by $\sin(\alpha_\phi)$ results in

$$\alpha_\phi = \arcsin\left(\frac{\sin(\alpha_\psi)\Omega_1 - \cos(\alpha_\psi)\Omega_2}{\sqrt{\boldsymbol{\Omega}^T\boldsymbol{\Omega}}}\right), \tag{44}$$

which is well defined since $|\sin(\alpha_\psi)\Omega_1 - \cos(\alpha_\psi)\Omega_2| \leq \sqrt{\Omega_1^2 + \Omega_2^2} < \sqrt{\boldsymbol{\Omega}^T\boldsymbol{\Omega}}$ due to $\Omega_3 \geq \Omega_3^* > 0$, see (41). Moreover, from the first equation of (43) we have

$$\alpha_\theta = \arctan\left(\frac{\cos(\alpha_\psi)\Omega_1 + \sin(\alpha_\psi)\Omega_2}{\Omega_3}\right), \tag{45}$$

which is also well defined since $\Omega_3 \geq \Omega_3^* > 0$, see (41). Substituting (39) into (38) results in

$$\dot{V}_2 = -\gamma\frac{\boldsymbol{\sigma}^T(\boldsymbol{\eta}_{1e})\boldsymbol{K}_1\boldsymbol{\sigma}(\boldsymbol{\eta}_{1e})}{\Delta(\boldsymbol{v}_1)} - \boldsymbol{v}_{1e}^T\boldsymbol{K}_2\boldsymbol{\sigma}(\boldsymbol{v}_{1e}) + \frac{1}{m}\boldsymbol{v}_{1e}^T\boldsymbol{G}_1\sqrt{\boldsymbol{\Omega}^T\boldsymbol{\Omega}}\boldsymbol{H}(\boldsymbol{q}_e, \boldsymbol{\alpha_q})\boldsymbol{e}_3. \tag{46}$$

Substituting (39) into (25) results in

$$\dot{\boldsymbol{v}}_{1e} = -\boldsymbol{K}_2\boldsymbol{\sigma}(\boldsymbol{v}_{1e}) - \gamma\boldsymbol{\sigma}(\boldsymbol{\eta}_{1e}) + \frac{1}{m}\boldsymbol{G}_1\sqrt{\boldsymbol{\Omega}^T\boldsymbol{\Omega}}\boldsymbol{H}(\boldsymbol{q}_e, \boldsymbol{\alpha_q})\boldsymbol{e}_3. \tag{47}$$

4.2. Stage 2

4.2.1. Step 1

We define

$$\boldsymbol{\omega}_e = \boldsymbol{\omega} - \boldsymbol{\alpha_\omega}, \tag{48}$$

where $\boldsymbol{\alpha_\omega}$ is a virtual control of $\boldsymbol{\omega}$. Before calculating $\dot{\boldsymbol{q}}_e$, let us calculate $\dot{\boldsymbol{\alpha_q}}$. From (36), we have

$$\dot{\boldsymbol{\alpha_q}} = \boldsymbol{K}(\boldsymbol{\alpha_q})\boldsymbol{\chi}, \tag{49}$$

where

$$\boldsymbol{K}(\boldsymbol{\alpha_q}) = \frac{1}{2}\begin{bmatrix} -\boldsymbol{\alpha}_{\bar{\boldsymbol{q}}}^T \\ \alpha_{q_0}\boldsymbol{I}_{3\times3} + \boldsymbol{S}(\alpha_{\bar{\boldsymbol{q}}}) \end{bmatrix},$$

$$\boldsymbol{\chi} = \begin{bmatrix} 1 & 0 & -\sin(\alpha_\theta) \\ 0 & \cos(\alpha_\phi) & \cos(\alpha_\theta)\sin(\alpha_\phi) \\ 0 & -\sin(\alpha_\phi) & \cos(\alpha_\theta)\cos(\alpha_\phi) \end{bmatrix} \begin{bmatrix} \frac{\partial\alpha_\phi}{\partial\boldsymbol{\eta}_1}\boldsymbol{v}_1 + \frac{\partial\alpha_\phi}{\partial\boldsymbol{v}_1}\Big(-g\boldsymbol{e}_3 + \frac{1}{m}f\boldsymbol{R}_1(\boldsymbol{q})\boldsymbol{e}_3\Big) + \sum_{i=1}^3 \frac{\partial\alpha_\phi}{\partial \overset{(i-1)}{\boldsymbol{\eta}_{1d}}}\overset{(i)}{\boldsymbol{\eta}_{1d}} + \frac{\partial\alpha_\phi}{\partial\psi_d}\dot{\psi}_d \\ \frac{\partial\alpha_\theta}{\partial\boldsymbol{\eta}_1}\boldsymbol{v}_1 + \frac{\partial\alpha_\theta}{\partial\boldsymbol{v}_1}\Big(-g\boldsymbol{e}_3 + \frac{1}{m}f\boldsymbol{R}_1(\boldsymbol{q})\boldsymbol{e}_3\Big) + \sum_{i=1}^3 \frac{\partial\alpha_\theta}{\partial \overset{(i-1)}{\boldsymbol{\eta}_{1d}}}\overset{(i)}{\boldsymbol{\eta}_{1d}} + \frac{\partial\alpha_\theta}{\partial\psi_d}\dot{\psi}_d \\ \dot{\psi}_d \end{bmatrix}. \tag{50}$$

Differentiating both sides of (31) along the solutions of (48), (49), and the third equation of (1) yields

$$\dot{\boldsymbol{q}}_e = \boldsymbol{K}(\boldsymbol{q})(\boldsymbol{\alpha_\omega} + \boldsymbol{\omega}_e) \pm \boldsymbol{K}(\boldsymbol{\alpha_q})\boldsymbol{\chi}. \tag{51}$$

Since there is the sign ambiguity in (51), which is resulted from the definition of $\boldsymbol{q}_e$, see (31), it is difficult to design the virtual control $\boldsymbol{\alpha_\omega}$ from (51) to stabilize $\boldsymbol{q}_e$ at the origin. Thus, we perform the following coordinate transformations

$$z_0 = \alpha_{q_0}q_0 + \boldsymbol{\alpha}_{\bar{\boldsymbol{q}}}^T\bar{\boldsymbol{q}}, \quad \bar{\boldsymbol{z}} = \alpha_{q_0}\bar{\boldsymbol{q}} - q_0\boldsymbol{\alpha}_{\bar{\boldsymbol{q}}} - \boldsymbol{S}(\boldsymbol{\alpha}_{\bar{\boldsymbol{q}}})\bar{\boldsymbol{q}}, \tag{52}$$

where α_{q_0} is the first element of $\boldsymbol{\alpha_q}$ and $\boldsymbol{\alpha}_{\bar{\boldsymbol{q}}}$ is the vector containing the second, third and fourth elements of $\boldsymbol{\alpha_q}$, i.e.,

$$\boldsymbol{\alpha_q} = [\alpha_{q_0} \ \boldsymbol{\alpha}_{\bar{\boldsymbol{q}}}^T]^T. \tag{53}$$

From (52), we have the following proposition:

Proposition 4..1 *The following implication holds:*

$$\begin{cases} \lim_{t\to\infty} z_0(t) = \pm 1 \\ \lim_{t\to\infty} \bar{\boldsymbol{z}}(t) = \boldsymbol{0} \end{cases} \Rightarrow \lim_{t\to\infty} \boldsymbol{q}_e(t) = 0. \tag{54}$$

Proof. See Appendix A. This proposition implies that designing the virtual control $\boldsymbol{\alpha}_{\boldsymbol{\omega}}$ to stabilize $\boldsymbol{q}_e$ at the origin is equivalent to designing $\boldsymbol{\alpha}_{\boldsymbol{\omega}}$ to stabilize z_0 at ± 1 and $\bar{\boldsymbol{z}}$ at the origin. As such, differentiating both sides of (52) along the solutions of (31), the third equation of (1), (48) and (51) yields

$$\dot{z}_0 = -\frac{1}{2}\bar{\boldsymbol{z}}^T(\boldsymbol{\alpha}_{\boldsymbol{\omega}} - \boldsymbol{\chi} + \boldsymbol{\omega}_e), \quad \dot{\bar{\boldsymbol{z}}} = \frac{1}{2}\boldsymbol{G}_2(\boldsymbol{\alpha}_{\boldsymbol{\omega}} - \boldsymbol{\chi} + \boldsymbol{\omega}_e), \tag{55}$$

where

$$\boldsymbol{G}_2 = z_0 \boldsymbol{I}_{3\times 3} + \boldsymbol{S}(\bar{\boldsymbol{z}}). \tag{56}$$

To design the virtual control $\boldsymbol{\alpha}_{\boldsymbol{\omega}}$, we consider the following Lyapunov function candidate

$$V_3 = \|\bar{\boldsymbol{z}}\|^2, \tag{57}$$

whose derivative along the solutions of the second equation of (55) satisfies

$$\dot{V}_3 = \bar{\boldsymbol{z}}^T \boldsymbol{G}_2(\boldsymbol{\alpha}_{\boldsymbol{\omega}} - \boldsymbol{\chi} + \boldsymbol{\omega}_e), \tag{58}$$

which suggests that we choose

$$\boldsymbol{\alpha}_{\boldsymbol{\omega}} = -k_3 \boldsymbol{G}_2^T \bar{\boldsymbol{z}} + \boldsymbol{\chi}, \tag{59}$$

where k_3 is a positive constant. It is noted that $\boldsymbol{\alpha}_{\boldsymbol{\omega}}$ is a smooth function of z_0, $\bar{\boldsymbol{z}}$, $\boldsymbol{\eta}_1$, $\boldsymbol{v}_1$, $\boldsymbol{q}$, $\boldsymbol{\eta}_{1d}$ $\dot{\boldsymbol{\eta}}_{1d}$, $\ddot{\boldsymbol{\eta}}_{1d}$, $\dddot{\boldsymbol{\eta}}_{1d}$, ψ_d, and $\dot{\psi}_d$. Substituting (59) into (58) gives

$$\dot{V}_3 = -k_3 \bar{\boldsymbol{z}}^T \boldsymbol{G}_2 \boldsymbol{G}_2^T \bar{\boldsymbol{z}} + \bar{\boldsymbol{z}}^T \boldsymbol{G}_2 \boldsymbol{\omega}_e. \tag{60}$$

Substituting (59) into (55) gives

$$\dot{z}_0 = \frac{k_3}{2}\bar{\boldsymbol{z}}^T \boldsymbol{G}_2^T \bar{\boldsymbol{z}} - \frac{1}{2}\bar{\boldsymbol{z}}^T \boldsymbol{\omega}_e, \quad \dot{\bar{\boldsymbol{z}}} = -\frac{k_3}{2}\boldsymbol{G}_2^T \bar{\boldsymbol{z}} + \frac{1}{2}\boldsymbol{G}_2 \boldsymbol{\omega}_e. \tag{61}$$

4.2.2. Step 2

This is the final step, in which we design the actual moment vector $\boldsymbol{\tau}$ to stabilize $\boldsymbol{\omega}_e$ at the origin. Differentiating both sides of (48) along the solutions of (48), (55) and (1) yields

$$\begin{aligned}\dot{\boldsymbol{\omega}}_e =& -\boldsymbol{J}^{-1}\boldsymbol{S}(\boldsymbol{\omega})\boldsymbol{J}\boldsymbol{\omega} + \boldsymbol{J}^{-1}\boldsymbol{\tau} - \frac{\partial \boldsymbol{\alpha}_{\boldsymbol{\omega}}}{\partial z_0}\Big(-\frac{1}{2}\bar{\boldsymbol{z}}^T(\boldsymbol{\alpha}_{\boldsymbol{\omega}} - \boldsymbol{\chi} + \boldsymbol{\omega}_e)\Big) - \frac{\partial \boldsymbol{\alpha}_{\boldsymbol{\omega}}}{\partial \bar{\boldsymbol{z}}}\Big(\frac{1}{2}\boldsymbol{G}_2(\boldsymbol{\alpha}_{\boldsymbol{\omega}} - \boldsymbol{\chi} + \boldsymbol{\omega}_e)\Big) \\ & - \frac{\partial \boldsymbol{\alpha}_{\boldsymbol{\omega}}}{\partial \boldsymbol{\eta}_1}\boldsymbol{v}_1 - \frac{\partial \boldsymbol{\alpha}_{\boldsymbol{\omega}}}{\partial \boldsymbol{v}_1}\Big(-g\boldsymbol{e}_3 + \frac{1}{m}f\boldsymbol{R}_1(\boldsymbol{q})\boldsymbol{e}_3\Big) - \frac{\partial \boldsymbol{\alpha}_{\boldsymbol{\omega}}}{\partial \boldsymbol{q}}\Big(\boldsymbol{K}(\boldsymbol{q})\boldsymbol{\omega}\Big) - \sum_{i=1}^{4}\frac{\partial \boldsymbol{\alpha}_{\boldsymbol{\omega}}}{\partial \overset{(i-1)}{\boldsymbol{\eta}_{1d}}}\overset{(i)}{\boldsymbol{\eta}_{1d}} - \sum_{i=1}^{2}\frac{\partial \boldsymbol{\alpha}_{\boldsymbol{\omega}}}{\partial \overset{(i-1)}{\psi_d}}\overset{(i)}{\psi_d},\end{aligned} \tag{62}$$

which suggests that we choose the control $\boldsymbol{\tau}$ as

$$\begin{aligned}\boldsymbol{\tau} =& -\boldsymbol{J}\boldsymbol{K}_4\boldsymbol{\omega}_e + \boldsymbol{S}(\boldsymbol{\omega})\boldsymbol{J}\boldsymbol{\omega} + \boldsymbol{J}\Bigg[\frac{\partial \boldsymbol{\alpha}_{\boldsymbol{\omega}}}{\partial z_0}\Big(-\frac{1}{2}\bar{\boldsymbol{z}}^T(\boldsymbol{\alpha}_{\boldsymbol{\omega}} - \boldsymbol{\chi} + \boldsymbol{\omega}_e)\Big) + \frac{\partial \boldsymbol{\alpha}_{\boldsymbol{\omega}}}{\partial \bar{\boldsymbol{z}}}\Big(\frac{1}{2}\boldsymbol{G}_2(\boldsymbol{\alpha}_{\boldsymbol{\omega}} - \boldsymbol{\chi} + \boldsymbol{\omega}_e)\Big) \\ & + \frac{\partial \boldsymbol{\alpha}_{\boldsymbol{\omega}}}{\partial \boldsymbol{\eta}_1}\boldsymbol{v}_1 + \frac{\partial \boldsymbol{\alpha}_{\boldsymbol{\omega}}}{\partial \boldsymbol{v}_1}\Big(-g\boldsymbol{e}_3 + \frac{1}{m}f\boldsymbol{R}_1(\boldsymbol{q})\boldsymbol{e}_3\Big) + \frac{\partial \boldsymbol{\alpha}_{\boldsymbol{\omega}}}{\partial \boldsymbol{q}}\Big(\boldsymbol{K}(\boldsymbol{q})\boldsymbol{\omega}\Big) + \sum_{i=1}^{4}\frac{\partial \boldsymbol{\alpha}_{\boldsymbol{\omega}}}{\partial \overset{(i-1)}{\boldsymbol{\eta}_{1d}}}\overset{(i)}{\boldsymbol{\eta}_{1d}} + \sum_{i=1}^{2}\frac{\partial \boldsymbol{\alpha}_{\boldsymbol{\omega}}}{\partial \overset{(i-1)}{\psi_d}}\overset{(i)}{\psi_d},\Bigg],\end{aligned} \tag{63}$$

where $\boldsymbol{K}_4$ is a positive definite matrix. Substituting (63) into (62) results in

$$\dot{\boldsymbol{\omega}}_e = -\boldsymbol{K}_4\boldsymbol{\omega}_e. \tag{64}$$

For convenience of stability analysis, we rewrite the closed loop system consisting of (24), (47), (61), and (64) as follows:

$$\begin{aligned}\dot{\boldsymbol{\eta}}_{1e} &= -\boldsymbol{K}_1\frac{\boldsymbol{\sigma}(\boldsymbol{\eta}_{1e})}{\Delta(\boldsymbol{v}_1)} + \boldsymbol{v}_{1e}, \\ \dot{\boldsymbol{v}}_{1e} &= -\boldsymbol{K}_2\boldsymbol{\sigma}(\boldsymbol{v}_{1e}) - \gamma\boldsymbol{\sigma}(\boldsymbol{\eta}_{1e}) + \frac{1}{m}\boldsymbol{G}_1\sqrt{\boldsymbol{\Omega}^T\boldsymbol{\Omega}}\boldsymbol{H}(\boldsymbol{q}_e, \boldsymbol{\alpha}_{\boldsymbol{q}})\boldsymbol{e}_3, \\ \dot{z}_0 &= \frac{k_3}{2}\bar{\boldsymbol{z}}^T\boldsymbol{G}_2^T\bar{\boldsymbol{z}} - \frac{1}{2}\bar{\boldsymbol{z}}^T\boldsymbol{\omega}_e, \\ \dot{\bar{\boldsymbol{z}}} &= -\frac{k_3}{2}\boldsymbol{G}_2^T\bar{\boldsymbol{z}} + \frac{1}{2}\boldsymbol{G}_2\boldsymbol{\omega}_e, \\ \dot{\boldsymbol{\omega}}_e &= -\boldsymbol{K}_4\boldsymbol{\omega}_e.\end{aligned} \tag{65}$$

The control design has been completed. We summarize the results in the following theorem.

Theorem 4..1 *Under the assumptions that the reference position trajectory $\boldsymbol{\eta}_{1d}(t)$ is sufficient smooth and satisfies the conditions (5) and (6) and that the reference yaw angle $\psi_d(t)$ is sufficiently smooth and satisfies the condition (7), the control laws consisting of (42) and (63) solve Control objective 2..1. In particular, the followings hold for all initial conditions $\boldsymbol{\eta}_1(t_0) \in \mathbb{R}^3$, $\boldsymbol{v}_1(t_0) \in \mathbb{R}^3$, $\boldsymbol{q}(t_0) \in \mathbb{R}^3$ with $\|\boldsymbol{q}(t_0)\|^2 = 1$, and $\boldsymbol{\omega}(t_0) \in \mathbb{R}^3$:*

1. *The actual control input f_i, $i = 1, \cdots, 4$ to the rotor i can be found by solving (3) with f and $\boldsymbol{\tau}$ given in (42) and (63), respectively, i.e.,*

$$\begin{bmatrix} f_1 \\ f_2 \\ f_3 \\ f_4 \end{bmatrix} = \begin{bmatrix} 1 & 1 & 1 & 1 \\ 0 & -L & 0 & L \\ -L & 0 & L & 0 \\ -C_a & C_a & -C_a & C_a \end{bmatrix}^{-1} \begin{bmatrix} f \\ \boldsymbol{\tau} \end{bmatrix}. \tag{66}$$

2. *The closed loop system (65) is forward complete.*
3. *The aircraft's position $\boldsymbol{\eta}_1(t)$ and the aircraft's yaw angle $\psi(t)$ of the aircraft globally asymptotically and locally exponentially track their reference trajectories $\boldsymbol{\eta}_{1d}(t)$ and $\psi_d(t)$.*
4. *All other states of the aircraft dynamics bounded.*

Proof. See Appendix B.

5. DEALING WITH UNMEASURED LINEAR VELOCITY AND DISTURBANCES

In Section 4., the control design was presented for the quadrotor aircraft with full-state available for feedback and without disturbances. In this section, we address the unmeasured linear velocity and the disturbance issues. For the unmeasured linear velocity problem, we provide a design of exponential observers for estimating the unmeasured linear velocity vector $\boldsymbol{v}_1$. For the disturbance problem, we include disturbance force and disturbance moment vectors in the quadrotor dynamics and design exponential observers for estimating these disturbance vectors. The control design can be then done by combining the control design in Section 4. with the exponential observers developed in this section.

5.1. Dealing with unmeasured linear velocity

This subsection develops an exponential observer to estimate the linear velocity $\boldsymbol{v}_1$ of the quadrotor aircraft. For convenience, we here rewrite the position dynamics of the aircraft, i.e., the first two equations of (1):

$$\begin{aligned} \dot{\boldsymbol{\eta}}_1 &= \boldsymbol{v}_1, \\ \dot{\boldsymbol{v}}_1 &= -g\boldsymbol{e}_3 + \frac{1}{m} f \boldsymbol{R}_1(\boldsymbol{q})\boldsymbol{e}_3. \end{aligned} \tag{67}$$

Since the second equation of (67) does not contain a damping term, designing an exponential observer for estimating $\boldsymbol{v}_1$ is slightly involved. Nevertheless, we propose the following observer:

$$\begin{aligned} \dot{\hat{\boldsymbol{\eta}}}_1 &= \boldsymbol{\chi} + \boldsymbol{K}_{01}(\boldsymbol{\eta}_1 - \hat{\boldsymbol{\eta}}_1), \\ \hat{\boldsymbol{v}}_1 &= \boldsymbol{\chi} + \boldsymbol{K}_{01}(\boldsymbol{\eta}_1 - \hat{\boldsymbol{\eta}}_1), \\ \dot{\boldsymbol{\chi}} &= -g\boldsymbol{e}_3 + \frac{1}{m} f \boldsymbol{R}_1(\boldsymbol{q})\boldsymbol{e}_3 + \boldsymbol{K}_{02}(\boldsymbol{\eta}_1 - \hat{\boldsymbol{\eta}}_1), \end{aligned} \tag{68}$$

where $\hat{\boldsymbol{\eta}}_1$ and $\hat{\boldsymbol{v}}_1$ denote estimates of $\boldsymbol{\eta}_1$ and $\boldsymbol{v}_1$, respectively, $\boldsymbol{K}_{01}$ and $\boldsymbol{K}_{02}$ are positive definite matrices. We now show that the observer (68) ensures that $\hat{\boldsymbol{\eta}}_1$ and $\hat{\boldsymbol{v}}_1$ exponentially tend to $\boldsymbol{\eta}_1$ and $\boldsymbol{v}_1$, respectively. To do so, let us define the following observer errors:

$$\begin{aligned} \tilde{\boldsymbol{\eta}}_1 &= \boldsymbol{\eta}_1 - \hat{\boldsymbol{\eta}}_1, \\ \tilde{\boldsymbol{v}}_1 &= \boldsymbol{v}_1 - \hat{\boldsymbol{v}}_1. \end{aligned} \tag{69}$$

Differentiating both sides of (69) along the solutions of (68) and (67) yields

$$\begin{aligned} \dot{\tilde{\boldsymbol{\eta}}}_1 &= \tilde{\boldsymbol{v}}_1, \\ \dot{\tilde{\boldsymbol{v}}}_1 &= -\boldsymbol{K}_{02}\tilde{\boldsymbol{\eta}}_1 - \boldsymbol{K}_{01}\tilde{\boldsymbol{v}}_1, \end{aligned} \tag{70}$$

which is globally exponentially stable at the origin because $\boldsymbol{K}_{01}$ and $\boldsymbol{K}_{02}$ are positive definite matrices.

5.2. Dealing with disturbances

The dynamics of the quadrotor aircraft subject to disturbances can be represented as:

$$\begin{cases} \dot{\boldsymbol{\eta}}_1 = \boldsymbol{v}_1, \\ \dot{\boldsymbol{v}}_1 = -g e_3 + \frac{1}{m} f \boldsymbol{R}_1(\boldsymbol{q}) e_3 + \frac{1}{m} \boldsymbol{F}_d, \end{cases} \quad \begin{cases} \dot{\boldsymbol{q}} = \boldsymbol{K}(\boldsymbol{q})\boldsymbol{\omega}, \\ \dot{\boldsymbol{\omega}} = -\boldsymbol{J}^{-1}\boldsymbol{S}(\boldsymbol{\omega})\boldsymbol{J}\boldsymbol{\omega} + \boldsymbol{J}^{-1}(\boldsymbol{\tau} + \boldsymbol{\tau}_d), \end{cases} \tag{71}$$

where $\boldsymbol{F}_d$ is the disturbance force vector coordinated in the earth-fixed frame and $\boldsymbol{\tau}_d$ is the disturbance moment vector coordinated in the body-fixed frame. The goal of this subsection is to design observers that exponentially estimate the disturbance vectors $\boldsymbol{F}_E$ and $\boldsymbol{\tau}_d$. To avoid repeating representation, we design an observer for exponentially estimating a disturbance vector in a general second-order nonlinear system, which covers the dynamics of the quadrotor aircraft (71). As such, we consider the following second-order system:

$$\begin{aligned} \dot{\boldsymbol{x}}_1 &= \boldsymbol{f}_1(t, \boldsymbol{x}_1, \boldsymbol{x}_2), \\ \dot{\boldsymbol{x}}_2 &= \boldsymbol{f}_2(t, \boldsymbol{x}_1, \boldsymbol{x}_2) + \boldsymbol{G}(t, \boldsymbol{x}_1)\boldsymbol{d}(t), \end{aligned} \tag{72}$$

where $t \in \mathbb{R}^+$, $\boldsymbol{x}_1 \in \mathbb{R}^n$, $\boldsymbol{x}_2 \in \mathbb{R}^n$, $\boldsymbol{f}_1(t, \boldsymbol{x}_1, \boldsymbol{x}_2)$ and $\boldsymbol{f}_2(t, \boldsymbol{x}_1, \boldsymbol{x}_2)$ are vectors of known functions of t, $\boldsymbol{x}_1$ and $\boldsymbol{x}_2$, $\boldsymbol{G}(t, \boldsymbol{x}_1)$ is a matrix whose elements are functions of t and $\boldsymbol{x}_1$, and $\boldsymbol{d}(t)$ is a vector of unknown disturbances. The system (72) satisfies the following assumption:

Assumption 5..1

1. *The disturbance vector $\boldsymbol{d}(t)$ and its derivative are bounded, i.e., there exist nonnegative constants d_M and d_{1M} such that $\|\boldsymbol{d}(t)\| \le d_M$ and $\|\dot{\boldsymbol{d}}(t)\| \le d_{1M}$, for all $t \ge t_0 \ge 0$, where $t_0 \ge 0$ is the initial time.*
2. *The system (72) is well-posed for all $t \ge t_0 \ge 0$.*
3. *The matrix $\boldsymbol{G}(t, \boldsymbol{x}_1)$ is invertible for all $t \ge t_0 \ge 0$ and $\boldsymbol{x}_1 \in \mathbb{R}^n$, and is differentiable with respect to t and $\boldsymbol{x}_1$.*

The disturbance observer is given in the following lemma.

Lemma 5..1 *Under Assumption 5..1, the disturbance observer $\hat{\boldsymbol{d}}$ of the disturbance $\boldsymbol{d}(t)$ is given by*

$$\begin{aligned} &\hat{\boldsymbol{d}} = \boldsymbol{\xi} + \boldsymbol{K}\boldsymbol{G}^{-1}(t, \boldsymbol{x}_1)\boldsymbol{x}_2, \\ &\dot{\boldsymbol{\xi}} = -\boldsymbol{K}\boldsymbol{\xi} - \boldsymbol{K}\Big(\frac{\partial \boldsymbol{G}^{-1}(t, \boldsymbol{x}_1)}{\partial t} + \frac{\partial \boldsymbol{G}^{-1}(t, \boldsymbol{x}_1)}{\partial \boldsymbol{x}_1}\boldsymbol{f}_1(t, \boldsymbol{x}_1, \boldsymbol{x}_2)\Big)\boldsymbol{x}_2 - \boldsymbol{K}\Big(\boldsymbol{G}^{-1}(t, \boldsymbol{x}_1)\boldsymbol{f}_2(t, \boldsymbol{x}_1, \boldsymbol{x}_2) + \boldsymbol{K}\boldsymbol{G}^{-1}(t, \boldsymbol{x}_1)\boldsymbol{x}_2\Big), \\ &\boldsymbol{\xi}(t_0) = -\boldsymbol{K}\boldsymbol{G}^{-1}(t_0, \boldsymbol{x}_1(t_0))\boldsymbol{x}_2(t_0), \end{aligned} \tag{73}$$

where $\boldsymbol{K}$ is a symmetric and positive definite matrix. The system (73) guarantees that the disturbance observer error $\boldsymbol{d}_e = \hat{\boldsymbol{d}} - \boldsymbol{d}$ and the disturbance observer $\hat{\boldsymbol{d}}$ satisfy the following properties:

$$\begin{aligned} \|\boldsymbol{d}_e(t)\| &\le \sqrt{\Big(\|\boldsymbol{d}(t_0)\|^2 - \frac{d_{1M}^2}{\lambda_m^2(\boldsymbol{K})}\Big)e^{-\lambda_m(\boldsymbol{K})(t-t_0)} + \frac{d_{1M}^2}{\lambda_m^2(\boldsymbol{K})}}, \\ \|\hat{\boldsymbol{d}}(t)\| &\le \frac{\lambda_M(\boldsymbol{K})}{\lambda_m(\boldsymbol{K})} d_M, \end{aligned} \tag{74}$$

for all $t \ge t_0 \ge 0$, where $\lambda_M(\boldsymbol{K})$ and $\lambda_m(\boldsymbol{K})$ are the maximum and minimum eigenvalues of $\boldsymbol{K}$, respectively.

Proof. See Appendix C.

Remark 5..1

1. *The system (73) is dynamical. The state $\boldsymbol{\xi}$ is generated by the second equation of (73), which is an ordinary differential equation, with the initial value $\boldsymbol{\xi}(t_0)$ chosen as in the third equation of (73). The choice of the matrix $\boldsymbol{K}$ directly affects performance of the disturbance observer. The larger eigenvalues of the matrix $\boldsymbol{K}$ give the faster the response of the disturbance observer.*

2. *The first inequality of (74) means that the disturbance observer error $\boldsymbol{d}_e(t)$ exponentially converges to a ball with a radius of $\frac{d_{1M}}{\lambda_m(\boldsymbol{K})}$ centered at the origin. The radius $\frac{d_{1M}}{\lambda_m(\boldsymbol{K})}$ can be made arbitrarily small by choosing a matrix $\boldsymbol{K}$ with a large minimum eigenvalue. In the case $d_{1M} = 0$, i.e., the constant disturbance, the disturbance observer error $\boldsymbol{d}_e(t)$ exponentially converges to zero. The second inequality of (74) gives the upper-bound of the disturbance observer $\hat{\boldsymbol{d}}(t)$. This upper-bound depends on the upper-bound of the disturbance $\boldsymbol{d}(t)$ and the matrix $\boldsymbol{K}$. If we choose $\boldsymbol{K}$ such that $\lambda_m(\boldsymbol{K}) = \lambda_M(\boldsymbol{K})$, then the upper-bound of the disturbance observer $\hat{\boldsymbol{d}}(t)$ will not exceed the upper-bound d_M of the disturbance $\boldsymbol{d}(t)$.*

3. *Continuality and differentiability of the disturbance observer $\hat{\boldsymbol{d}}(t)$ depend only on those of $\boldsymbol{f}_1(t, \boldsymbol{x}_1, \boldsymbol{x}_2)$, $\boldsymbol{f}_2(t, \boldsymbol{x}_1, \boldsymbol{x}_2)$, and $\boldsymbol{G}(t, \boldsymbol{x}_1)$.*

Applying Lemma 5..1 to (71) results in the following observers for exponentially estimating $\boldsymbol{F}_d$ and $\boldsymbol{\tau}_d$:

$$\begin{cases} \hat{\boldsymbol{F}}_d = \boldsymbol{\xi}_1 + m\boldsymbol{K}_{d1}\boldsymbol{v}_1, \\ \dot{\boldsymbol{\xi}}_1 = -\boldsymbol{K}_{d1}\boldsymbol{\xi}_1 - \boldsymbol{K}_{d1}\big(-mg\boldsymbol{e}_3 + f\boldsymbol{R}_1(\boldsymbol{q})\boldsymbol{e}_3 + m\boldsymbol{K}_{1d}\boldsymbol{v}_1\big), \\ \boldsymbol{\xi}_1(t_0) = -m\boldsymbol{K}_{d1}\boldsymbol{v}_1(t_0), \end{cases}$$
$$\begin{cases} \hat{\boldsymbol{\tau}}_d = \boldsymbol{\xi}_2 + \boldsymbol{K}_{d2}\boldsymbol{J}\boldsymbol{\omega}, \\ \dot{\boldsymbol{\xi}}_2 = -\boldsymbol{K}_{d2}\boldsymbol{\xi}_2 - \boldsymbol{K}_{d2}\big(-\boldsymbol{S}(\boldsymbol{\omega})\boldsymbol{J}\boldsymbol{\omega} + \boldsymbol{\tau} + \boldsymbol{K}_{d2}\boldsymbol{J}\boldsymbol{\omega}\big), \\ \boldsymbol{\xi}_2(t_0) = -\boldsymbol{K}_{d2}\boldsymbol{J}\boldsymbol{\omega}(t_0), \end{cases} \tag{75}$$

where $\boldsymbol{K}_{d1}$ and $\boldsymbol{K}_{d2}$ are diagonal and positive definite matrices. The observers (75) guarantee that the observer errors $\boldsymbol{F}_{de} = \hat{\boldsymbol{F}}_d - \boldsymbol{F}_d$ and $\boldsymbol{\tau}_{de} = \hat{\boldsymbol{\tau}}_d - \boldsymbol{\tau}_d$, and the observers $\hat{\boldsymbol{F}}_d$ and $\hat{\boldsymbol{\tau}}_d$ satisfy

$$\begin{cases} \|\boldsymbol{F}_{de}(t)\| \le \sqrt{\left(\|\boldsymbol{F}_d(t_0)\|^2 - \frac{F_{1dM}^2}{\lambda_m^2(\boldsymbol{K}_{d1})}\right)\mathrm{e}^{-\lambda_m(\boldsymbol{K}_{d1})(t-t_0)} + \frac{F_{1dM}^2}{\lambda_m^2(\boldsymbol{K}_{d1})}}, \\ \|\hat{\boldsymbol{F}}_d(t)\| \le \frac{\lambda_M(\boldsymbol{K}_{d1})}{\lambda_m(\boldsymbol{K}_{d1})}F_{dM}, \end{cases}$$
$$\begin{cases} \|\boldsymbol{\tau}_{de}(t)\| \le \sqrt{\left(\|\boldsymbol{\tau}_d(t_0)\|^2 - \frac{\tau_{1dM}^2}{\lambda_m^2(\boldsymbol{K}_{d2})}\right)\mathrm{e}^{-\lambda_m(\boldsymbol{K}_{d2})(t-t_0)} + \frac{\tau_{1dM}^2}{\lambda_m^2(\boldsymbol{K}_{d2})}}, \\ \|\hat{\boldsymbol{\tau}}_d(t)\| \le \frac{\lambda_M(\boldsymbol{K}_{d2})}{\lambda_m(\boldsymbol{K}_{d2})}\tau_{dM}, \end{cases} \tag{76}$$

for all $t \ge t_0 \ge 0$, where F_{dM} and F_{1dM} are the upper bounds of $\|\boldsymbol{F}_d\|$ and $\|\dot{\boldsymbol{F}}_d\|$, respectively, and τ_{dM} and τ_{1dM} are the upper bounds of $\|\boldsymbol{\tau}_d\|$ and $\|\dot{\boldsymbol{\tau}}_d\|$, respectively. It is noted from (76) that the disturbance observer errors $\boldsymbol{F}_{de}$ and $\boldsymbol{\tau}_{de}$ exponentially converge to balls, which are centered at the origin and have radii of $\frac{F_{1dM}}{\lambda_m(\boldsymbol{K}_{d1})}$ and $\frac{\tau_{1dM}}{\lambda_m(\boldsymbol{K}_{d2})}$, respectively. These radii can be made arbitrarily small by choosing the matrices $\boldsymbol{K}_{d1}$ and $\boldsymbol{K}_{d2}$ with sufficiently large $\lambda_m(\boldsymbol{K}_{d1})$ and $\lambda_m(\boldsymbol{K}_{d2})$, respectively. Indeed, if $\boldsymbol{F}_d$ and $\boldsymbol{\tau}_d$ are constant we have $F_{1dM} = \tau_{1dM} = 0$, i.e., the disturbance observer errors $\boldsymbol{F}_{de}$ and $\boldsymbol{\tau}_{de}$ exponentially converge zero. Moreover, the disturbance estimates $\hat{\boldsymbol{F}}_d$ and $\hat{\boldsymbol{\tau}}_d$ are upper bounded by $\frac{\lambda_M(\boldsymbol{K}_{d1})}{\lambda_m(\boldsymbol{K}_{d1})}F_{dM}$ and $\frac{\lambda_M(\boldsymbol{K}_{d2})}{\lambda_m(\boldsymbol{K}_{d2})}\tau_{dM}$, respectively. In addition, let $\boldsymbol{F}_d = [F_{xd}\ F_{yd}\ F_{zd}]^T$, $\hat{\boldsymbol{F}}_d = [\hat{F}_{xd}\ \hat{F}_{yd}\ \hat{F}_{zd}]^T$, and F_{xdM}, F_{ydM}, and F_{zdM} be the upper bounds of $|F_{xd}|$, $|F_{yd}|$, and $|F_{zd}|$, respectively. Then we have $|\hat{F}_{xd}| \le \frac{\lambda_M(\boldsymbol{K}_{d1})}{\lambda_m(\boldsymbol{K}_{d1})}F_{xdM}$, $|\hat{F}_{yd}| \le \frac{\lambda_M(\boldsymbol{K}_{d1})}{\lambda_m(\boldsymbol{K}_{d1})}F_{ydM}$, and $|\hat{F}_{zd}| \le \frac{\lambda_M(\boldsymbol{K}_{d1})}{\lambda_m(\boldsymbol{K}_{d1})}F_{zdM}$ because the matrix $\boldsymbol{K}_{1d}$ is diagonal.

The above linear velocity and disturbance observers ensure that the control design presented in Section 4. is straightforwardly extended to handle the unmeasured linear velocity and disturbance problems. The only note to take is that the condition (6) is replaced by

$$\sup_{t\in\mathbb{R}^+} |\ddot{z}_{1d}(t)| \le g - \varrho_5 - \frac{\lambda_M(\boldsymbol{K}_{d1})}{\lambda_m(\boldsymbol{K}_{d1})}F_{zdM}. \tag{77}$$

This condition implies that the aircraft is not desirable to land or to take-off faster than it freely falls under gravity and the disturbance force in the vertical direction.

6. SIMULATION RESULTS

In this section, we illustrate the effectiveness of the proposed global tracking controller through a numerical simulation. The aircraft's parameters are taken as $m = 0.5$kg, $L = 0.25$m, $C_a = 0.05$m, $g = 9.81\text{m}/s^2$, and $\boldsymbol{J} = 10^{-3}\text{diag}(5, 5, 9)\text{kg}/\text{m}^2$. The reference trajectories are taken as $\boldsymbol{\eta}_{1d}(t) = [10\sin(0.01t)\ 10\cos(0.01t)\ 0.1t]^T$, and $\psi_d(t) = 0.01t$. The smooth saturation function $\sigma(\bullet)$ is chosen as $\sigma(\bullet) = \tanh(\bullet)$. The control gains are chosen as $\boldsymbol{K}_1 = \boldsymbol{K}_2 = 0.5\boldsymbol{I}_{3\times3}$, $k_3 = 5$, $\boldsymbol{K}_4 = 10\boldsymbol{I}_{3\times3}$, and $\gamma = 0.5$.

It can be verified that the conditions (28) and (41) hold. The initial conditions are $\boldsymbol{\eta}_1(0) = [5\ 1\ 1]^T$, $\boldsymbol{v}_1(0) = [0\ 0\ 0]^T$, $\boldsymbol{q}(0) = [0.883\ 0.3\ -0.2\ -0.3]^T$, and $\boldsymbol{\omega}(0) = [0\ 0\ 0]^T$. The position reference trajectory $\boldsymbol{\eta}_{1d}$ and the position real trajectory $\boldsymbol{\eta}_1$ are plotted in Figure 1. The position and attitude tracking errors and control forces are plotted in Figure 2. It is seen from these figures that all tracking errors asymptotically converge to zero. Noticing that it takes longer time for the position tracking error vector $\boldsymbol{\eta}_{1e}(t)$ to converge to zero than for the attitude tracking error vector $\boldsymbol{q}_e$ since we need to choose sufficiently small gain matrices $\boldsymbol{K}_1$ and $\boldsymbol{K}_2$ so that the conditions (28) and (41) hold.

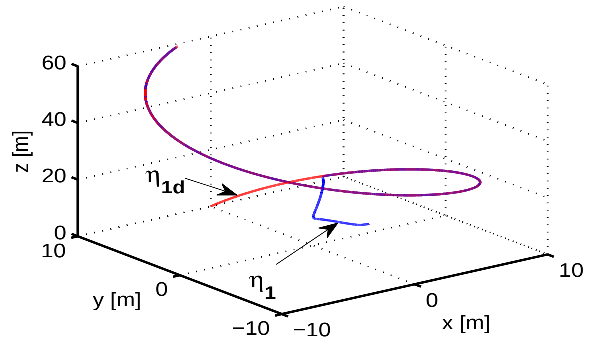

Figure 1. Reference and real position trajectories $\boldsymbol{\eta}_{1d}$ and $\boldsymbol{\eta}_1$

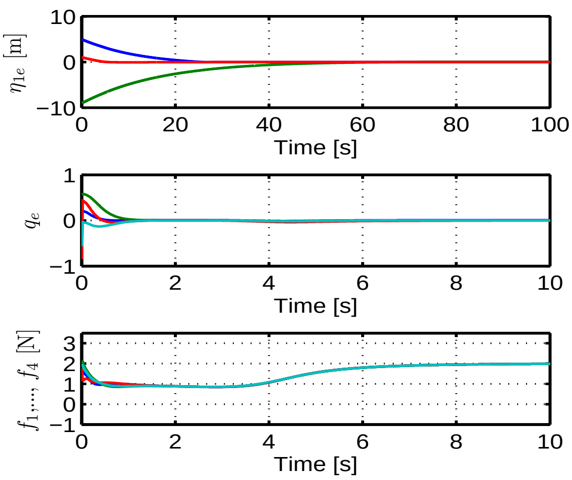

Figure 2. Position and attitude tracking errors, and control forces

7. CONCLUSIONS

The attractive points of this paper include the combination of the Euler angles and unit-quaternion for the aircraft's attitude representation, and the one-step backstepping ahead. These features can be applied to design global tracking controllers for underactuated ocean and land vehicles in the future.

A PROOF OF PROPOSITION 4.1

Noticing from (52) that $z_0 = \boldsymbol{\alpha}_{\boldsymbol{q}}^T\boldsymbol{q}$ and from (36) that $\|\boldsymbol{\alpha}_{\boldsymbol{q}}\|^2 = 1$, therefore the case where $z_0 = 1$ and $\bar{\boldsymbol{z}} = \boldsymbol{0}$ corresponds to the minus sign in (31) and the case where $z_0 = -1$ and $\bar{\boldsymbol{z}} = \boldsymbol{0}$ corresponds to the plus sign in (31). We only consider the case where $\lim_{t\to\infty} z_0(t) = 1$ and $\lim_{t\to\infty} \bar{\boldsymbol{z}}(t) = \boldsymbol{0}$. The case where $\lim_{t\to\infty} z_0(t) = -1$ and $\lim_{t\to\infty} \bar{\boldsymbol{z}}(t) = \boldsymbol{0}$ can be carried out in the same manner. Moreover, it is sufficient to take $z_0 = 1$ and $\bar{\boldsymbol{z}} = \boldsymbol{0}$ the instead of their limits since $z_0(t)$ and $\bar{\boldsymbol{z}}(t)$ are bounded (recall that $z_0^2(t) + \|\bar{\boldsymbol{z}}(t)\|^2 = 1$ for all $t \geq t_0 \geq 0$). Using $\boldsymbol{\alpha}_{\boldsymbol{q}} = \boldsymbol{q} - \boldsymbol{q}_e$ from (31), we can write z_0 and $\bar{\boldsymbol{z}}$ defined in (52) in terms of $\boldsymbol{q}_e$ as follows:

$$\begin{aligned} z_0 &= 1 - \boldsymbol{q}^T\boldsymbol{q}_e, \\ \bar{\boldsymbol{z}} &= -q_{0e}\bar{\boldsymbol{q}} + q_0\bar{\boldsymbol{q}}_e - \boldsymbol{S}(\bar{\boldsymbol{q}}_e)\bar{\boldsymbol{q}}. \end{aligned} \tag{78}$$

We consider two separate cases where $q_0 \neq 0$ and $q_0 = 0$. For the case where $q_0 \neq 0$, setting $z_0 = 1$ and $\bar{\boldsymbol{z}} = \boldsymbol{0}$ in (78), and multiplying both sides of the second equation of (78) by $\bar{\boldsymbol{q}}_e^T$ give

$$\left\{ \begin{array}{c} \bar{\boldsymbol{q}}^T\bar{\boldsymbol{q}}_e + q_0 q_{0e} = 0 \\ -q_{0e}\bar{\boldsymbol{q}}_e^T\bar{\boldsymbol{q}} + q_0\bar{\boldsymbol{q}}_e^T\bar{\boldsymbol{q}}_e = 0 \end{array} \right. \Rightarrow q_0\boldsymbol{q}_e^T\boldsymbol{q}_e = 0, \tag{79}$$

which yields $\boldsymbol{q}_e = \boldsymbol{0}$ since $q_0 \neq 0$ for this case. For the case where $q_0 = 0$, setting $z_0 = 1$ and $\bar{\boldsymbol{z}} = \boldsymbol{0}$ in (78), and multiplying both sides of the second equation of (78) by $\bar{\boldsymbol{q}}^T$ give

$$\left\{ \begin{array}{c} \bar{\boldsymbol{q}}^T\bar{\boldsymbol{q}}_e = 0 \\ -q_{0e}\bar{\boldsymbol{q}}^T\bar{\boldsymbol{q}} = 0 \end{array} \right. \Rightarrow q_0\boldsymbol{q}^T\boldsymbol{q} = 0. \tag{80}$$

Since $q_0 = 0$ for this case and $\boldsymbol{q}^T\boldsymbol{q} = 1$, we have $\bar{\boldsymbol{q}}^T\bar{\boldsymbol{q}} = 1$. This implies from (80) that $q_{0e} = 0$. We now need to show that $\bar{\boldsymbol{q}}_e = \boldsymbol{0}$. Since we have already shown that $q_{0e} = 0$ and are considering the case where $q_0 = 0$, the second equation of (78) with $\bar{\boldsymbol{z}} = \mathbf{0}$ gives $\boldsymbol{S}(\bar{\boldsymbol{q}}_e)\bar{\boldsymbol{q}} = \mathbf{0}$. This equation and the first equation of (80) mean that the dot and cross products of the two vectors $\bar{\boldsymbol{q}}_e$ and $\bar{\boldsymbol{q}}$ are both equal to zero while $\|\bar{\boldsymbol{q}}\| = 1$. Therefore, we must have $\bar{\boldsymbol{q}}_e = \mathbf{0}$. □

B PROOF OF THEOREM 4.1

To prove Theorem 4..1, we first show that the closed loop system (65) is forward complete. Second, we consider the last equation of the closed loop system to show that $\boldsymbol{\omega}_e(t)$ exponentially converges to zero. Third, we prove that $\bar{\boldsymbol{z}}(t)$ and $z_0(t)$ asymptotically tend to $\mathbf{0}$ and ± 1, respectively. Fourth, we show that $\boldsymbol{\eta}_{1e}(t)$ and $\boldsymbol{v}_{1e}(t)$ asymptotically converge to zero. Last, we prove that all other states of the aircraft dynamics bounded.

B1. Proof of forward completeness of the closed loop system and exponential convergence of $\boldsymbol{\omega}_e(t)$

To prove that the closed loop system (65) is forward complete, we consider the following function

$$\varphi_1 = \sqrt{1 + V_2} + z_0^2 + V_3 + \frac{\xi_0}{2}\|\boldsymbol{\omega}_e\|^2, \tag{81}$$

where V_2 is given in (37) with V_1 defined in (19), and ξ_0 is a positive constant to be selected. It is seen that φ_1 is positive definite and radially unbounded in $\boldsymbol{\eta}_{1e}$, $\boldsymbol{v}_{1e}$, z_0, $\bar{\boldsymbol{z}}$, and $\boldsymbol{\omega}_e$. It can be shown that the first derivative of φ_1 with respect to time along the solutions of (46), the third equation of the closed loop system (65), (60), and the last equation of the closed loop system (65) satisfies

$$\begin{aligned}\dot{\varphi}_1 =& \frac{1}{\sqrt{1+V_2}}\Big[-\gamma\frac{\boldsymbol{\sigma}^T(\boldsymbol{\eta}_{1e})\boldsymbol{K}_1\boldsymbol{\sigma}(\boldsymbol{\eta}_{1e})}{\Delta(\boldsymbol{v}_1)} - \boldsymbol{v}_{1e}^T\boldsymbol{K}_2\boldsymbol{\sigma}(\boldsymbol{v}_{1e}) + \frac{1}{m}\boldsymbol{v}_{1e}^T\boldsymbol{G}_1\sqrt{\boldsymbol{\Omega}^T\boldsymbol{\Omega}}\boldsymbol{H}(\boldsymbol{q}_e,\boldsymbol{\alpha_q})\boldsymbol{e}_3\Big] + \\ & \frac{k_3}{2}\bar{\boldsymbol{z}}^T\boldsymbol{G}_2^T\bar{\boldsymbol{z}}z_0 - \frac{1}{2}\bar{\boldsymbol{z}}^T\boldsymbol{\omega}_e z_0 - k_3\bar{\boldsymbol{z}}^T\boldsymbol{G}_2\boldsymbol{G}_2^T\bar{\boldsymbol{z}} + \bar{\boldsymbol{z}}^T\boldsymbol{G}_2\boldsymbol{\omega}_e - \xi_0\boldsymbol{\omega}_e^T\boldsymbol{K}_4\boldsymbol{\omega}_e\end{aligned} \tag{82}$$

Using the expressions of $\boldsymbol{G}_1$ in (26), $\boldsymbol{G}_2$ in (56), $\boldsymbol{H}(\boldsymbol{q}_e,\boldsymbol{\alpha_q})$ in (32) or in (33), and the bound of the elements Ω_1, Ω_2, and Ω_3 of $\boldsymbol{\Omega}$ defined in (40), we have

$$\|\boldsymbol{G}_1\| \le 1 + \|\boldsymbol{K}_1\|,\ \|\boldsymbol{G}_2\| \le 2,\ \|\boldsymbol{H}(\boldsymbol{q}_e,\boldsymbol{\alpha_q})\| \le 2,\ \sqrt{\boldsymbol{\Omega}^T\boldsymbol{\Omega}} \le \sqrt{\Omega_{1M}^2 + \Omega_{2M}^2 + \Omega_{3M}^2}. \tag{83}$$

Using (83) and the fact that $z_0^2 + \bar{\boldsymbol{z}}^T\bar{\boldsymbol{z}} = 1$, we can bound $\dot{\varphi}$ as follows:

$$\dot{\varphi}_1 \le -M_1\|\boldsymbol{\omega}_e\|^2 + M_2, \tag{84}$$

where

$$\begin{aligned}M_1 &= 2\Big(\xi_0\lambda_m(\boldsymbol{K}_4) - \frac{5}{4}\Big), \\ M_2 &= \frac{5}{4} + \frac{1}{m}2\sqrt{2}(1 + \|\boldsymbol{K}_1\|)\sqrt{\Omega_{1M}^2 + \Omega_{2M}^2 + \Omega_{3M}^2},\end{aligned} \tag{85}$$

where $\lambda_m(\boldsymbol{K}_4)$ is the minimum eigenvalue of $\boldsymbol{K}_4$. Hence picking $\xi_0 \ge \frac{5}{4\lambda_m(\boldsymbol{K}_4)}$ results in $\dot{\varphi}_1 \le M_2$, which together with φ_1 defined in (81) implies that the closed loop system (65) is forward complete.

Since we have already proved that the closed loop system (65) is forward complete, to show that $\boldsymbol{\omega}_e(t)$ exponentially converges to zero we can consider the last equation of the closed loop system (65) separately. As such, we consider the function $V_4 = \frac{1}{2}\|\boldsymbol{\omega}_e\|^2$ whose derivative along the solutions of the last equation of the closed loop system (65) is $\dot{V}_4 = -\boldsymbol{\omega}_e^T\boldsymbol{K}_4\boldsymbol{\omega}_e$, which implies that $\boldsymbol{\omega}_e(t)$ exponentially converges to zero since $\boldsymbol{K}_4$ is a positive definite matrix.

B2. Proof of asymptotic convergence of $z_0(t)$ and $\bar{\boldsymbol{z}}(t)$

To show that $\lim_{t\to\infty} z_0(t) = \pm 1$ and $\lim_{t\to\infty} \bar{\boldsymbol{z}}(t) = \mathbf{0}$, we consider $V_0 = z_0^2$ and V_3 defined in (57) to obtain

$$\mathcal{Z}_0)\begin{cases} V_0 = z_0^2 \\ \dot{V}_0 = k_3 z_0^2\|\bar{\boldsymbol{z}}\|^2 - z_0\bar{\boldsymbol{z}}^T\boldsymbol{\omega}_e \end{cases},\quad \bar{\boldsymbol{\mathcal{Z}}})\begin{cases} V_3 = \|\bar{\boldsymbol{z}}\|^2 \\ \dot{V}_3 = -k_3 z_0^2\|\bar{\boldsymbol{z}}\|^2 + \bar{\boldsymbol{z}}^T\boldsymbol{G}_2\boldsymbol{\omega}_e, \end{cases} \tag{86}$$

where we have used (60), the third equation of the closed loop system (65). Using the fact that we have already proved that $\boldsymbol{\omega}_e(t)$ exponentially converges to zero, and that $z_0(t)$ and $\bar{\boldsymbol{z}}(t)$ are bounded (since $z_0^2(t) + \|\bar{\boldsymbol{z}}(t)\|^2 = 1$ for all

$t \geq t_0 \geq 0$), instead of considering (86) to study asymptotic convergence of $z_0(t)$ and $\bar{\boldsymbol{z}}(t)$ we can consider the following equations

$$\mathcal{Z}_0^*) \left\{ \begin{array}{l} V_0^* = z_0^2 \\ \dot{V}_0^* = k_3 z_0^2 \|\bar{\boldsymbol{z}}\|^2 \end{array} \right. , \quad \bar{\boldsymbol{\mathcal{Z}}}^*) \left\{ \begin{array}{l} V_3^* = \|\bar{\boldsymbol{z}}\|^2 \\ \dot{V}_3^* = -k_3 z_0^2 \|\bar{\boldsymbol{z}}\|^2. \end{array} \right. \tag{87}$$

The subsystem $\mathcal{Z}_0^*$ is unstable. Instability of the subsystem $\mathcal{Z}_0^*$ implies that $z_0(t)$ asymptotically tends to a non-zero but bounded value if $z_0(t_0) \neq 0$. If $z_0(t_0) = 0$, arbitrarily small noise will drive $z_0(t_0)$ to a non-zero value $z_0(t)$ at some t since the subsystem $\mathcal{Z}_0^*$ is unstable. A non-zero $z_0(t)$ implies from the subsystem $\bar{\boldsymbol{\mathcal{Z}}}^*$ that $\bar{\boldsymbol{z}}(t)$ tends to zero asymptotically. Since $z_0^2(t) + \|\bar{\boldsymbol{z}}(t)\|^2 = 1$, $z_0(t)$ will eventually converge to 1 or -1. Asymptotic convergence of $z_0(t)$ to ± 1 and $\bar{\boldsymbol{z}}(t)$ to $\mathbf{0}$ implies from Proposition 4..1 that $\boldsymbol{q}_e(t)$ asymptotically converge to $\mathbf{0}$.

B3. Proof of asymptotic convergence of $\boldsymbol{\eta}_{1e}(t)$ and $\boldsymbol{v}_{1e}(t)$

To prove asymptotic convergence of $\boldsymbol{\eta}_{1e}(t)$ and $\boldsymbol{v}_{1e}(t)$ to zero, we consider the following Lyapunov function candidate

$$V_2^* = 2\sqrt{1 + V_2}, \tag{88}$$

whose derivative along the solutions of (46)

$$\dot{V}_2^* = -\frac{1}{\sqrt{1 + V_2}} \left(\gamma \frac{\boldsymbol{\sigma}^T(\boldsymbol{\eta}_{1e}) \boldsymbol{K}_1 \boldsymbol{\sigma}(\boldsymbol{\eta}_{1e})}{\Delta(\boldsymbol{v}_1)} + \boldsymbol{v}_{1e}^T \boldsymbol{K}_2 \boldsymbol{\sigma}(\boldsymbol{v}_{1e}) \right) + \varpi \boldsymbol{H}(\boldsymbol{q}_e, \boldsymbol{\alpha}_{\boldsymbol{q}}) \boldsymbol{e}_3, \tag{89}$$

where $\varpi = \frac{1}{\sqrt{1+V_2}} \frac{1}{m} \boldsymbol{v}_{1e}^T \boldsymbol{G}_1 \sqrt{\boldsymbol{\Omega}^T \boldsymbol{\Omega}}$. We need to show that the term ϖ is bounded by a constant. As such, using V_2 in (37), $\boldsymbol{G}_1$ in (26), and the bound of the elements Ω_1, Ω_2, and Ω_3 of $\boldsymbol{\Omega}$ defined in (40), we can calculate the bound of ϖ as follows:

$$\varpi = \frac{1}{m} \frac{\boldsymbol{v}_{1e}^T \boldsymbol{G}_1 \sqrt{\boldsymbol{\Omega}^T \boldsymbol{\Omega}}}{\sqrt{1 + \gamma V_1 + \frac{1}{2}\|\boldsymbol{v}_{1e}\|^2}} \leq \frac{1}{m} \frac{\|\boldsymbol{v}_{1e}\| \|\boldsymbol{G}_1\| \sqrt{\boldsymbol{\Omega}^T \boldsymbol{\Omega}}}{\sqrt{1 + \gamma V_1 + \frac{1}{2}\|\boldsymbol{v}_{1e}\|^2}} \leq \frac{1}{m} \sqrt{2}(1 + \|\boldsymbol{K}_1\|) \sqrt{\Omega_{1M}^2 + \Omega_{2M}^2 + \Omega_{3M}^2}. \tag{90}$$

We now use the fact that the term $\varpi(t)$ is bounded as shown above for all $t \geq t_0 \geq 0$ and that $\lim_{t\to\infty} \boldsymbol{q}_e(t) = 0$ as proved above. Moreover, the limit $\lim_{t\to\infty} \boldsymbol{q}_e(t) = 0$ implies that $\lim_{t\to\infty} \boldsymbol{H}(\boldsymbol{q}_e(t), \boldsymbol{\alpha}_{\boldsymbol{q}}(t)) = 0$, see the expression of $\boldsymbol{H}(\boldsymbol{q}_e, \boldsymbol{\alpha}_{\boldsymbol{q}})$ in (33). The limit $\lim_{t\to\infty} \boldsymbol{H}(\boldsymbol{q}_e(t), \boldsymbol{\alpha}_{\boldsymbol{q}}(t)) = 0$ in turn implies that $\lim_{t\to\infty} [\varpi(t)\, \boldsymbol{H}(\boldsymbol{q}_e(t), \boldsymbol{\alpha}_{\boldsymbol{q}}(t)) \boldsymbol{e}_3] = 0$. Integrating both sides of (89) and utilizing the limit $\lim_{t\to\infty} \varpi(t) \boldsymbol{H}(\boldsymbol{q}_e(t), \boldsymbol{\alpha}_{\boldsymbol{q}}(t)) \boldsymbol{e}_3 = 0$ show that $V_2(t)$ or $V_2^*(t)$ is bounded for all $t \geq t_0 \geq 0$. Boundedness of $V_2(t)$ or $V_2^*(t)$ implies boundedness of $\boldsymbol{\eta}_{1e}(t)$, $\boldsymbol{v}_{1e}(t)$, and $\boldsymbol{v}_1(t)$ (see (17) and note that $\boldsymbol{\alpha}_{\boldsymbol{v}_1}$ is bounded for all $t \geq t_0 \geq 0$). In addition, by construction all the signals $\boldsymbol{\eta}_{1e}(t)$, $\boldsymbol{v}_{1e}(t)$, and $\boldsymbol{v}_1(t)$ are continuous. The aforementioned arguments imply from (88) and (89) that $\lim_{t\to\infty} \big(\gamma \frac{\boldsymbol{\sigma}^T(\boldsymbol{\eta}_{1e}(t)) \boldsymbol{K}_1 \boldsymbol{\sigma}(\boldsymbol{\eta}_{1e}(t))}{\Delta(\boldsymbol{v}_1(t))} + \boldsymbol{v}_{1e}^T(t) \boldsymbol{K}_2 \boldsymbol{\sigma}(\boldsymbol{v}_{1e}(t)) \big) = 0$, which in turn means that $\lim_{t\to\infty} (\boldsymbol{\eta}_{1e}(t), \boldsymbol{v}_{1e}(t)) = 0$ since $\boldsymbol{v}_1(t)$ is bounded. Asymptotic convergence of $\psi(t) - \psi_d(t)$ to zero is resulted from that of $\boldsymbol{q}_e(t)$ to zero.

We now show that the closed loop system (65) is locally exponentially stable at the origin. Since we have already asymptotic stability of the close loop system (65), there exists a time $T \geq t_0$ such that $\Delta(\boldsymbol{v}_1(t)) \leq \Delta(\dot{\boldsymbol{\eta}}_{1d}(t) + \varepsilon_0$, $\boldsymbol{\sigma}(\boldsymbol{\eta}_{1e}(t)) \approx \boldsymbol{\eta}_{1e}(t)$, and $\boldsymbol{\sigma}(\boldsymbol{v}_{1e}(t)) \approx \boldsymbol{v}_{1e}(t)$, for all $t \geq T$. From these observations, local exponential stability of the closed loop system (65) follows.

Finally, boundedness of all other aircraft's states follows directly from the proposed smooth control design and boundedness of $\boldsymbol{\eta}_{1e}(t)$, $\boldsymbol{v}_{1e}(t)$, and the reference trajectories and their derivatives. □

C PROOF OF LEMMA 5.1

To prove the first inequality of (74) in Lemma 5..1, we differentiate the disturbance observer error $\boldsymbol{d}_e$ along the solutions of (73) to obtain

$$\dot{\boldsymbol{d}}_e = -\boldsymbol{K} \boldsymbol{d}_e + \dot{\boldsymbol{d}}. \tag{91}$$

Consider the function

$$V_e = \frac{1}{2} \|\boldsymbol{d}_e\|^2, \tag{92}$$

whose derivative along the solutions of (91) satisfies

$$\begin{aligned} \dot{V}_e &= -\boldsymbol{d}_e^T \boldsymbol{K} \boldsymbol{d}_e + \boldsymbol{d}_e^T \dot{\boldsymbol{d}}, \\ &\leq -\lambda_m(\boldsymbol{K}) V_e + \frac{d_{1M}^2}{2\lambda_m(\boldsymbol{K})}, \end{aligned} \tag{93}$$

where d_{1M} is defined in Assumption 5..1.1. The last inequality of (93) can be written as

$$\frac{\mathrm{d}}{\mathrm{d}t}\left(V_e - \frac{d_{1M}^2}{2\lambda_m^2(\boldsymbol{K})}\right) \leq -\lambda_m(\boldsymbol{K})\left(V_e - \frac{d_{1M}^2}{2\lambda_m^2(\boldsymbol{K})}\right). \tag{94}$$

Solving (94) gives

$$V_e(t) \leq \left(V_e(t_0) - \frac{d_{1M}^2}{2\lambda_m^2(\boldsymbol{K})}\right)\mathrm{e}^{-\lambda_m(\boldsymbol{K})(t-t_0)} + \frac{d_{1M}^2}{2\lambda_m^2(\boldsymbol{K})},\ \forall\, t \geq t_0 \geq 0, \tag{95}$$

which gives the first inequality of (74) by using the definition of V_e in (92) and the initial condition $\boldsymbol{\xi}(t_0)$ defined in the third equation of (73) implies that $\hat{\boldsymbol{d}}(t_0) = 0$.

To prove the second inequality of (74), we differentiate the disturbance observer $\hat{\boldsymbol{d}}$ defined in the first equation of (73) along the solutions of the second equation of (73) and (72) to obtain

$$\dot{\hat{\boldsymbol{d}}} = -\boldsymbol{K}\hat{\boldsymbol{d}} - \boldsymbol{K}\boldsymbol{d}. \tag{96}$$

Consider the following function

$$V = \frac{1}{2}\|\hat{\boldsymbol{d}}\|^2, \tag{97}$$

whose derivative along the solutions of (96) satisfies

$$\begin{aligned} \dot{V} &= -\hat{\boldsymbol{d}}^T\boldsymbol{K}\hat{\boldsymbol{d}} + \hat{\boldsymbol{d}}^T\boldsymbol{K}\boldsymbol{d}, \\ &\leq -\lambda_m(\boldsymbol{K})V + \frac{\lambda_M^2(\boldsymbol{K})}{2\lambda_m(\boldsymbol{K})}d_M^2, \end{aligned} \tag{98}$$

where d_M is defined in Assumption 5..1.1. Solving the last inequality of (98) gives

$$V(t) \leq \left(V(t_0) - \frac{\lambda_M^2(\boldsymbol{K})}{2\lambda_m^2(\boldsymbol{K})}d_M^2\right)\mathrm{e}^{-\lambda_m(\boldsymbol{K})(t-t_0)} + \frac{\lambda_M^2(\boldsymbol{K})}{2\lambda_m^2(\boldsymbol{K})}d_M^2,\ \forall\, t \geq t_0 \geq 0, \tag{99}$$

The initial condition $\boldsymbol{\xi}(t_0)$ defined in the third equation of (73) implies that $\hat{\boldsymbol{d}}(t_0) = 0$, which results in $V(t_0) = 0$. Substituting $V(t_0) = 0$ into (99) and using the definition of V in (97) result in the second inequality of (74). □

REFERENCES

[1] K. D. Do and J. Pan, *Control of Ships and Underwater Vehicles: Design for Underactuated and Nonlinear Marine Systems*. Springer, 2009.

[2] P. Kokotovic and M. Arcak, "Constructive nonlinear control: a history perspective," *Automatica*, vol. 37, no. 5, pp. 637–662, 2001.

[3] J. Hauser, S. Sastry, and G. Meyer, "Nonlinear control design for slightly non-minimum phase systems: application to v/stol aircraft," *Automatica*, vol. 28, no. 4, pp. 665–679, 1992.

[4] C.-S. Huang and K. Yuan, "Output tracking of a nonlinear non-minimum phase PVTOL aircraft based on nonlinear state feedback," *International Journal of Control*, vol. 75, no. 6, pp. 466–473, 2002.

[5] F. Lin, W. Zhang, and R. Brandt, "Robust hovering control of a PVTOL aircraft," *IEEE Transactions on Control Systems Technology*, vol. 7, no. 3, pp. 343–351, 1999.

[6] C. J. Tomlin and S. S. Sastry, "Bounded tracking for non-minimum phase nonlinear systems with fast zero dynamics," *International Journal of Control*, vol. 68, no. 4, pp. 819–847, 1997.

[7] P. Martin, S. Devasia, and B. Paden, "A different look at output tracking control of a VTOL aircraft," *Automatica*, vol. 32, no. 1, pp. 101–107, 1996.

[8] R. Olfati-Saber, "Global configuration stabilization for the VTOL aircraft with strong input coupling," *IEEE Transactions on Automatic Control*, vol. 47, no. 11, pp. 1949–1952, 2002.

[9] K. D. Do, Z. P. Jiang, and J. Pan, "Global tracking control of a VTOL aircraft without velocity measurements," *IEEE Transactions on Automatic Control*, vol. 48, no. 12, pp. 2212–2217, 2003.

[10] P. Setlur, D. Dawson, Y. Fang, and B. Costic, "Nonlinear tracking control of the VTOL aircraft," *Proceedings of the 40th IEEE Conference on Decision and Control, Florida USA*, pp. 4592–4597, 2001.

[11] H. Khalil, *Nonlinear Systems*. Prentice Hall, 2002.

[12] A. R. Teel, "Global stabilization and restricted tracking for multiple integrators with bounded control," *Systems and Control Letters*, vol. 18, no. 3, pp. 165–171, 1992.
[13] M. Krstic, I. Kanellakopoulos, and P. Kokotovic, *Nonlinear and Adaptive Control Design*. New York: Wiley, 1995.
[14] P. Castillo, A. Dzul, and R. Lozano, "Real-time stabilization and tracking of a four-rotor mini rotorcraft," *IEEE Transactions on Control Systems Technology*, vol. 12, no. 4, pp. 510–516, 2004.
[15] T. Madani and A. Benallegue, "Control of a quadrotor mini-helicopter via full state backstepping technique," *Proceedings of the 45th IEEE Conference on Decision & Control*, pp. 1515–1520, 2006.
[16] Z. Zuo, "Trajectory tracking control design with command-filtered compensation for a quadrotor," *IET Control Theory and Applications*, vol. 4, no. 11, pp. 1515–1520, 2010.
[17] M. D. Shuster, "A survey of attitude representations," *The Journal of the Astronautical Sciences*, vol. 41, no. 4, pp. 439–517, 1993.
[18] S. M. Joshi, A. G.Kelkar, and J. T.-Y.Wen, "Robust attitude stabilization of spacecraft using nonlinear quaternion feedback," *IEEE Transactions on Automatic Control*, vol. 40, no. 10, pp. 1800–1803, 1995.
[19] A. Tayebi and S. McGilvray, "Attitude stabilization of a VTOL quadrotor aircraft," *IEEE Transactions on Control Systems Technology*, vol. 14, no. 3, pp. 562–571, 2006.
[20] A. P. Aguiar and J. P. Hespanha, "Position tracking of underactuated vehicles," *Proceedings of American Control Conference*, vol. 3, pp. 1988–1993, 2003.
[21] A. Abdessameud and A. Tayebi, "Global trajectory tracking control of VTOL-UAVs without linear velocity measurements," *Automatica*, vol. 46, pp. 1053–1059, 2010.
[22] A. Roberts and A. Tayebi, "Adaptive position tracking of VTOL UAVs," *IEEE Transactions on Robotics*, vol. 27, no. 1, pp. 129–142, 2011.
[23] W. Dixon, M. de Queiroz, F. Zhang, and D. Dawson, "Tracking control of robot manipulators with bounded torque inputs," *Robotica*, vol. 17, no. 2, pp. 121–129, 1999.
[24] J. M. Godhavn, T. I. Fossen, and S. Berge, "Nonlinear and adaptive backstepping designs for tracking control of ships," *International Journal of Adaptive Control and Signal Processing*, vol. 12, no. 8, pp. 649–670, 1998.
[25] T. I. Fossen, *Guidance and Control of Ocean Vehicles*. John Wiley and Sons Ltd., 1994.
[26] N. Marchand and A. Hably, "Global stabilization of multiple integrators with bounded controls," *Automatica*, vol. 41, no. 12, pp. 2147–2152, 2005.
[27] Z. Lin, "Global control of linear systems with saturating actuators," *Automatica*, vol. 34, no. 7, pp. 897–905, 1998.

BIOGRAPHY OF AUTHOR

Khac Duc Do received the M.E. and Ph.D. degrees (with Distinction) in mechanical engineering from The University of Wollongong, Wollongong, Australia, and The University of Western Australia, Crawley, Australia, in 1999 and 2003, respectively. Until 2012, He was a Research Professor with the School of Mechanical Engineering, The University of Western Australia. He is currently an Associate Professor with the Department of Mechanical Engineering, Curtin University. His research interests include control of nonlinear systems, control of multiple agents, control of land, air, and ocean vehicles, and control of systems governed by partial differential equations. Further info on his homepage: http://mech-eng.curtin.edu.au/people/index.cfm/Duc